IVYSPRING INTERNATIONAL PUBLISHER

JOURNAL OF CANCER

2026; 17(12): 2019-2041. doi: 10.7150/jca.143340

Review

# Tumor Treating Fields in Solid Tumors: A Multiscale Evidence Framework with Gastric Cancer as an Early Translational Case Study

Yiwei Yuan[1], Haohan Zheng[1], Yipeng Zhang[2], Yulong Sun[3], Jianfeng Zhang[4]✉, Huijuan Li[2,3]✉

1. School of Automation and Information Engineering, Xi'an University of Technology, Xi'an, 710048, China.
2. School of Electrical Engineering, Shaanxi Polytechnic University, Xianyang, 712000, China.
3. School of Life Science and Technology, Northwestern Polytechnical University, Xi'an 710072, China.
4. School of Information Engineering, Hangzhou Medical College, Hangzhou, 311121 China.

✉ Corresponding authors: Jianfeng Zhang. Email: jianfeng3883@126.com; Huijuan Li. Email: lihuijuan@mail.nwpu.edu.cn.

© 2026 The Author(s). This is an open access article distributed under the Creative Commons Attribution 4.0 International Licence, subject to the Publisher's Terms of Use at https://ivyspring.com/terms.

Received: 2026.08.29; Accepted: 2026.10.22; Published: 2026.11.05

## Abstract

Tumor Treating Fields (TTFields) involve low-intensity, intermediate-frequency alternating electric fields and are most established for glioblastoma. Evidence for other solid tumors is growing, but data for gastric cancer remains limited to a single *in vitro* FOLFOX-combination study and an exploratory signal from the EF-31 single-arm study, which was reported in a registry and conference abstract without a peer-reviewed patient-outcome paper. We assess multiscale TTFields evidence in solid tumors, using gastric cancer as an early translational case study. For each scale, we differentiate between measured data and cross-scale inferences using a four-level mechanistic and cross-scale grading scheme (L0–L3: phenomenological observation, quantitative dose–response, mechanistic anchoring, and cross-scale predictive bridging), while recording clinical trial design, endpoints, and regulatory status on a separate clinical track. Retrospective glioblastoma analyses associate modeled dose with survival, but adherence-weighted metrics remain susceptible to confounding and do not establish a causal cross-scale link. However, most mechanisms at the molecular, immune, and resistance levels are supported only within individual scales rather than across the entire causal pathway. Therefore, gastric cancer should be viewed as an early stage for translational research rather than a fully established indication. Priorities include site-specific extracranial dosimetry, independently validated biomarkers, prospective dose-response studies, controlled combination trials, and careful management of adherence issues, device burden, and evidence concentration within a single commercial ecosystem.

Keywords: tumor treating fields; bioelectric-mechanical coupling; single-cell multi-omics; dosimetry; evidence maturity; gastric cancer

## 1. Introduction

Treating abdominal and thoracic solid tumors remains challenging, with limited survival improvements despite advances in surgery, radiotherapy, and systemic treatments. Tumor Treating Fields (TTFields) use wearable transducer arrays to deliver low-intensity (1–3 V/cm), intermediate-frequency (100–300 kHz) alternating electric fields. These physically target dividing cells without relying on drugs, avoiding the pharmacokinetic and systemic toxicity issues associated with chemotherapy [1, 2]. While randomized evidence supports clinical benefit in selected indications, the intervening causal pathways remain incompletely resolved. This review examines multiscale TTFields evidence across solid tumors, with gastric cancer as an early translational case study rather than an established indication. We distinguish clinical outcomes from evidence linking field distribution to cellular and molecular mechanisms.

The clinical evidence for TTFields is based on key randomized studies (Table 1). In recurrent glioblastoma (GBM), the EF-11 trial demonstrated survival rates similar to those achieved with physician's-choice chemotherapy, along with

improved quality of life, which supported regulatory approval in 2011 [3]. The EF-14 study then assessed TTFields combined with maintenance temozolomide versus temozolomide alone in newly diagnosed GBM. The median overall survival (OS) was 20.9 months with TTFields versus 16.0 months without, and progression-free survival (PFS) was 6.7 versus 4.0 months [4, 5]. As a result, TTFields has become part of the standard treatment for newly diagnosed GBM. Additional studies outside the brain include STELLAR for malignant pleural mesothelioma [6], LUNAR for metastatic non-small-cell lung cancer (NSCLC) [7], PANOVA-3 for locally advanced pancreatic adenocarcinoma [8], and METIS after stereotactic radiosurgery for brain metastases. Because tissue types, fluid spaces, and geometries vary across these sites, results from intracranial studies cannot be directly applied to thoracic or abdominal conditions without specific site calibration.

Evidence for gastric cancer remains preliminary. The peer-reviewed full-text study concerns AGS and KATO III cells rather than patient outcomes. At 150 kHz for 72 h, TTFields alone yielded cell counts of 53% and 57%, colony-forming ability of 62% and 41%, and source-reported composite overall effects of 37% and 24% of control in AGS (1.1 V/cm RMS) and KATO III (1.7 V/cm RMS) cells, respectively [9]. Adding FOLFOX further decreased viable cells. Mechanistic findings included downregulation of the Fanconi anaemia/BRCA pathway and increased γH2AX [9]. The interaction was described as additive, with a slight tendency toward synergy in AGS cells and toward antagonism in KATO III cells. Clinically, there is one exploratory study, not two independent ones. The phase II EF-31/ZL-8301-001 study (ClinicalTrials.gov NCT04281576 and the Annals of Oncology LBA3 abstract) enrolled 28 patients and is marked as completed, but reports "No Results Posted" as of 24 July 2026 [10]. LBA3 presented exploratory results for first-line TTFields plus XELOX in unresectable gastric or gastro-oesophageal junction adenocarcinoma [11]. These records are complementary and do not constitute independent evidence. "No Results Posted" indicates just the absence of a structured results report in the registry. The available data show clinical exploration has occurred but do not substitute for a full peer-reviewed patient-outcome report or prove TTFields' added benefit over XELOX. Within our two-track framework, the peer-reviewed mechanistic evidence for gastric cancer is preclinical L1, whereas clinical evidence remains limited to an exploratory single-arm phase II signal from the single EF-31 study.

The terminology needs a clear boundary. TTFields are continuous, low-intensity alternating fields in the 100–300 kHz range that primarily act during mitosis. In contrast, nanosecond pulsed electric fields and irreversible electroporation employ much stronger fields to permeabilize or destroy cell membranes and should not be interpreted as working through the same mechanism [12]. We use TTFields when referring to the Optune-type modality, whereas "alternating electric fields" encompasses the broader physical category. The optimal frequency varies by cell type—around 200 kHz for glioma lines—and efficacy improves at a delivered field intensity near 1 V/cm [2].

**Table 1:** Key clinical evidence and regulatory milestones for TTFields in solid tumors

| Trial/study | Indication | Design | TTFields regimen | Main outcome | Status/approval |
|---|---|---|---|---|---|
| EF-11 [3] | Recurrent glioblastoma | Randomized phase 3 | NovoTTF-100A monotherapy vs physician's-choice chemotherapy | Median OS comparable (HR 0.86, 95% CI 0.66–1.12; p=0.27); better quality of life; fewer adverse events | FDA PMA approval, 8 April 2011 (P100034); recurrent GBM monotherapy |
| EF-14 [4, 5] | Newly diagnosed glioblastoma | Randomized phase 3 | TTFields plus maintenance temozolomide vs temozolomide | Median OS 20.9 vs 16.0 months (HR 0.63, 95% CI 0.53–0.76; p<0.001); PFS 6.7 vs 4.0 months | FDA PMA supplement approval, 5 October 2015 (P100034/S013); newly diagnosed GBM with temozolomide |
| STELLAR [6] | Unresectable malignant pleural mesothelioma | Single-arm phase 2 | TTFields plus pemetrexed and platinum, first-line | Median OS 18.2 months (95% CI 12.1–25.8); no additional systemic toxicity | FDA HDE approval, 23 May 2019 (H180002); with pemetrexed and platinum-based chemotherapy |
| LUNAR [7] | Metastatic NSCLC after platinum | Randomized pivotal phase 3 | TTFields plus standard systemic therapy vs systemic therapy | Median OS 13.2 vs 9.9 months (95% CI 10.3–15.5 vs 8.1–11.5) | FDA PMA approval, 15 October 2024 (P230042); metastatic NSCLC after platinum-based therapy, with PD-1/PD-L1 inhibitors or docetaxel |
| PANOVA-3 [8] | Locally advanced pancreatic adenocarcinoma | Randomized phase 3 | TTFields plus gemcitabine/nab-paclitaxel vs gemcitabine/nab-paclitaxel | Median OS 16.2 vs 14.2 months (HR 0.82, 95% CI 0.68–0.99) | FDA PMA approval, 11 February 2026 (P250034); locally advanced pancreatic cancer with gemcitabine and nab-paclitaxel |
| METIS [118] | Brain metastases from NSCLC after SRS | Randomized phase 3 | TTFields after SRS vs SRS alone | Longer time to intracranial progression (HR 0.72, 95% CI 0.53–0.98; p=0.044) | Phase 3 final results (2026) |

Footnote: HR, hazard ratio; SRS, stereotactic radiosurgery; HDE, Humanitarian Device Exemption; PMA, premarket approval. Regulatory sources: U.S. Food and Drug Administration (FDA), PMA P100034, PMA supplement P100034/S013, HDE H180002, PMA P230042, and PMA P250034 (official database records; accessed 6 October 2026). Approval dates refer to the listed decisions. HDE and PMA are distinct regulatory pathways.

Early studies on the mechanism primarily examined the mitotic spindle. It was proposed that intermediate-frequency fields could act dielectrophoretically on polar tubulin dimers and septin complexes, disrupting spindle formation and chromosome segregation, which could lead to mitotic catastrophe [1, 2]. Subsequent research revealed effects such as replication stress, compromised DNA repair, autophagy, endoplasmic-reticulum stress, increased membrane permeability, immunogenic cell death, and activation of innate immunity [13-16]. These results suggest a multi-mechanism explanation; however, most research focuses on a single biological scale and does not demonstrate how these mechanisms form a continuous causal sequence.

We therefore examine macroscopic field physics, mesoscale mechanobiology, and microscale multi-omics all within a single framework. Few studies directly link a computed field distribution to a single-cell transcriptional change and patient survival. The evidence is organized into macroscopic field fingerprints (Section 2), nanomechanical feedback (Section 3), microscale multi-omic fingerprints (Section 4), signaling-circuit rewiring and resistance (Section 5), and physicochemical sensitization across barriers (Section 6). At each level, we consider what can be measured and whether that measurement predicts an outcome at the next scale. Figure 1 illustrates this structure, with field intensity and frequency on the horizontal axis and biological scale on the vertical axis.

This is a mechanistic narrative review. Literature searches, full-text assessments, and regulatory updates were completed as of 24 July 2026. The search targeted TTFields or intermediate-frequency, low-intensity alternating electric fields, tumor dosimetry, gastric and abdominal solid-tumor translation, single-cell readouts, and combination therapies. Nanosecond pulsed electric fields, irreversible electroporation, and magnetic-field therapies were not combined with TTFields. Sources included PubMed, PMC, Crossref, doi.org, ClinicalTrials.gov, FDA device databases, and the full-text PDFs stored in this project. Manuscript claims were based on papers with verified full texts and titles or DOIs, or official registry and regulatory records. Records only with abstracts, unavailable full texts, or unresolved titles or DOIs remain in the screening list. This review is not a PRISMA systematic review and does not provide pooled effect estimates. Search strategies, full-text matrices, and citation audit files have been archived for review.

This review examines TTFields evidence across dosimetry, cellular mechanics, molecular responses, and clinical outcomes in solid tumors. Gastric cancer serves as an early translational case study for testing how far findings from other tumor settings can be carried, rather than as an indication with an established clinical evidence base. We distinguish mechanistic and cross-scale evidence from clinical study design and regulatory status, and identify the gaps that limit their integration.

The Scale-Maturity Grading system (Box 1) separates mechanistic and cross-scale evidence into four levels—phenomenological observation (L0), quantitative dose–response (L1), mechanistic anchoring (L2), and cross-scale predictive bridging (L3)—while tracking clinical trial design, endpoints, and regulatory status separately rather than as a fifth mechanistic rung. Section 7 applies this two-track structure across indications, preventing clinical survival benefit from being treated as retrospective proof of a specific cellular mechanism, and Section 8 discusses key methodological limitations, including sham-control constraints for wearable devices and adherence-related confounding.

## 2. Macroscopic field signatures: tissue diversity, body-fluid interactions, and dose measurement

The primary identifiable pattern at the largest scale is the field distribution itself, showing where the alternating field concentrates, where it diminishes, and how consistently a planned dose reaches the tumor bed. Unlike a drug that circulates, an electric field is determined solely by the tissues' geometry and electrical properties, making the larger-scale challenge essentially about conductivity mapping and field calculation rather than pharmacokinetics.

### 2.1 Dielectric properties of tissue as the basis for field distribution

Any field calculation begins with understanding how biological tissues conduct within the TTFields operating range. The key reference is still the Gabriel parametric survey, which measured and modeled the dielectric spectrum of human tissues from 10 Hz to 20 GHz. It fitted a four-dispersion Cole–Cole model that provides the frequency-dependent conductivity and permittivity values used in nearly all TTFields simulations [17-19]. At around 200 kHz, different tissues vary in conductivity by more than an order of magnitude. Because the field tends to concentrate in more conductive compartments, this heterogeneity, rather than the applied voltage alone, determines the local dose. Studies have shown that intracranial field strength depends significantly on the assumed dielectric properties and anatomy: changing conductivity assignments or anatomical boundaries can substantially alter the modeled field strength.

Consequently, patient-specific property mapping, rather than a single homogeneous estimate, is now essential for accurate dosimetry [20].

## 2.2 Finite element modeling and patient-specific analysis

Numerical models translate dielectric properties into spatial field maps. Early studies with individualized head models showed that segmented MRI could predict field distributions in GBM, with electrode placement significantly influencing outcomes [21]. This approach was later formalized into a computational framework that relates the applied macroscopic field to the local cellular field [22]. Diffusion-tensor-derived conductivity tensors effectively capture anisotropy in white matter and muscle, affecting both field strength and direction, which is crucial when field orientation relative to the spindle axis impacts the mechanism (Section 3.1) [20].

Modeling has also expanded to target deeper extracranial areas; for example, pancreatic models reveal that attenuation limits coverage, but array optimization can enhance it [23], and automated pipelines now generate personalized simulations with minimal manual segmentation [24]. Recent lung studies combined modeling with experimental validation at 150 kHz. Using orthogonal arrays, lower-lung coverage in the Ella model increased from about 79.9% to 99.4%, and whole-lung coverage from 93.1% to 99.4%; in the Duke model, lower-lung coverage rose from roughly 88.2% to 99.9%, and whole-lung coverage from 93.3% to 96.9% [25]. A review of personalized computation highlights that anatomical segmentation, dielectric parameters, thermal safety, and adaptive planning are key constraints for reliable delivery [26]. Phantom measurements that reproduce simulated voltages support initial validation [27], but patient-specific spatial field verification remains impractical at present.

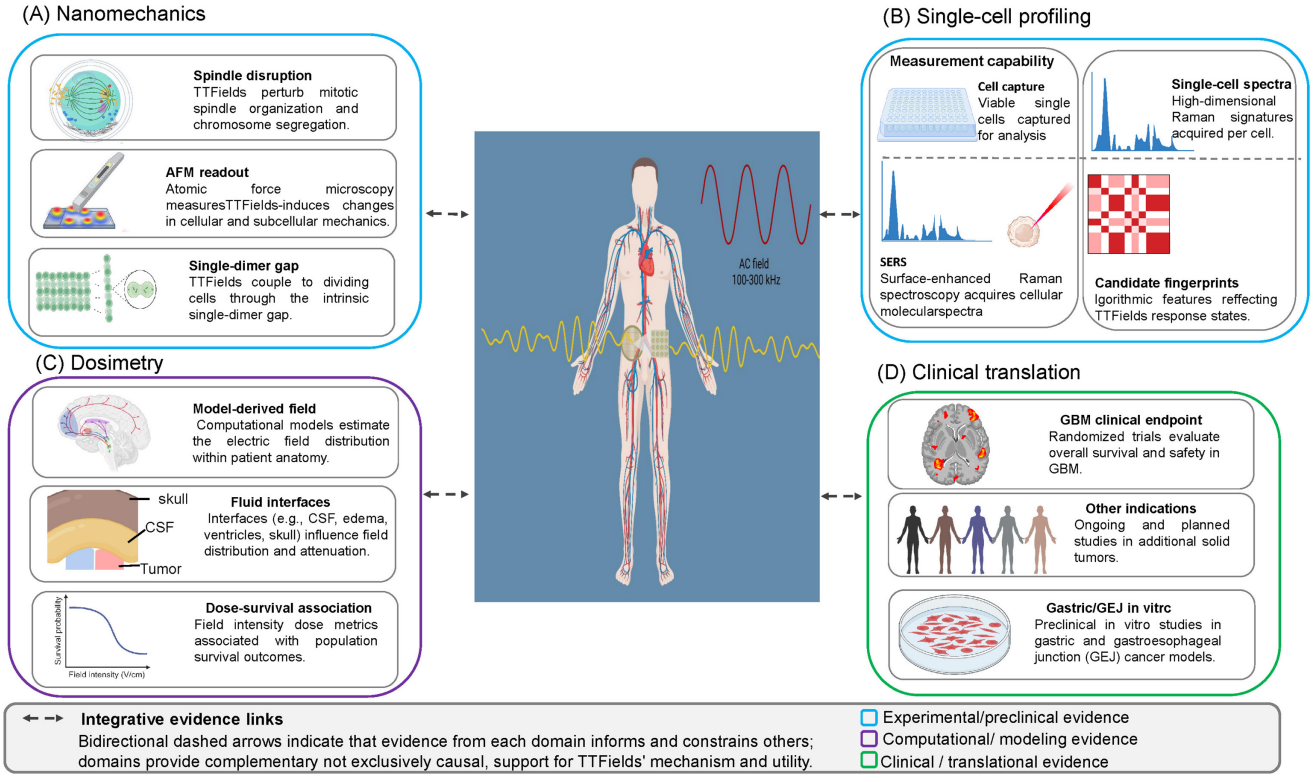



**Figure 1:** Cross-scale evidence architecture of TTFields. (A) Nanomechanics compiles cell-level evidence relevant to TTFields, including spindle disruption, nanomechanical measurements using AFM, and the single-dimer-gap concept related to dividing cells. (B) Single-cell profiling separates measurement methods from the actual readouts, showing cell capture, SERS data collection, single-cell spectra, and potential fingerprints linked to TTFields response states. (C) Dosimetry emphasizes computational and anatomical factors affecting field exposure, such as model-based field distribution, the role of fluid interfaces, and dose–survival correlation metrics. (D) Clinical translation depicts key contexts, including randomized studies in glioblastoma, other solid-tumor indications under investigation, and exploratory *in vitro* research in gastric/gastroesophageal-junction (GEJ) models. Dashed bidirectional arrows illustrate evidence connections across domains rather than direct causal pathways. The color coding differentiates experimental/preclinical, computational/modeling, and clinical/translational evidence.

### 2.3 Modulation of body fluids within complex cavities

Conductive fluid compartments and insulating gas pockets can markedly redistribute electric fields at tissue interfaces. Modeling and synthesis across anatomical sites indicate that cerebrospinal fluid, edema, urine, ascites, pleural fluid, and necrotic tumor cores alter TTFields propagation in a geometry-dependent manner [28], and realistic three-dimensional rat glioma models confirm that peritumoral edema, tumor size, and tumor location substantially affect local field strength and distribution [29]. Extending these principles to gastric and gastroesophageal junction tumors introduces pronounced, time-varying dielectric heterogeneity that a single static anatomical model cannot capture. Within the stomach lumen, variable volumes of high-ionic-strength gastric secretions and ingested liquids act as high-conductivity pathways that can shunt electric current away from adjacent mural segments, whereas swallowed air and intraluminal gas pockets form low-conductivity voids that deflect field lines and create local dose shadows or interface hotspots. Continuous peristaltic waves, posture shifts, respiratory motion, meal-related distension, and pathological ascites further alter gastric wall thickness and the spatial relationship between the primary tumor, perigastric fat planes, and regional lymph node stations. Moreover, although 1 V/cm is widely cited from preclinical and glioblastoma modeling as a convenient reference level for reporting simulated target coverage, it has not been clinically validated as a therapeutic efficacy threshold for gastric cancer. Consequently, current static torso simulations cannot guarantee uniform or temporally stable therapeutic field coverage across the full gastric wall and regional lymphatic drainage. These gastric-specific effects are physical expectations rather than direct measurements; their magnitude and direction depend on anatomy, array configuration, and boundary conditions.

A practical research direction is to extend abdominal planning from a single anatomy to a set of time-dependent anatomical states. Respiratory-resolved four-dimensional computed tomography (4D-CT), where justified, or dynamic magnetic resonance imaging (MRI) could characterize organ motion; separate acquisitions under standardized fasting and postprandial conditions could assess slower changes in gastric filling. Ascites and nonperiodic peristalsis would require additional scenarios because respiratory phase bins do not capture all abdominal variation. The gastric wall, tumor, luminal contents, major organs, and fluid compartments should be segmented for each state, with sensitivity analyses for uncertain dielectric properties. State-specific electric-field and thermal calculations could then quantify the range of tumor coverage and skin-heating constraints. Array layouts could be optimized for robustness across these scenarios, followed by repeat imaging when anatomy changes substantially. A dynamic phantom and independent measurements should test the workflow before prospective evaluation. These steps are proposed validation tasks; their ability to improve delivered abdominal TTFields exposure or patient outcomes remains unproven.

### 2.4 Dosimetry and the relationship between dose and survival

The clinical importance of these field calculations was demonstrated through a retrospective analysis of the EF-14 cohort. The relevant metric is local minimum dose density (LMiDD). In the original analysis, local minimum power density (LMiPD) was the lower power-loss density of the two field directions at each location. LMiDD was obtained by multiplying LMiPD by device-use compliance, and its average within the tumor bed was used for the outcome analysis [30]. Thus, LMiDD incorporates both modeled electrical exposure and device use; it is not simply $\sigma |E|^2$ or the spatial minimum across the tumor. The resulting dose estimates depend on the assumed dielectric properties and the recorded compliance. The original analysis included multivariable adjustment, but residual confounding related to health status, treatment tolerance, and device use remains possible. Because LMiDD multiplies modeled LMiPD by device-use compliance, its association with survival is not an adherence-independent causal dose effect [30]. In a simulation-based analysis of 340 EF-14 participants, higher tumor-bed LMiDD ($\geq 0.77$ mW/cm$^3$) was associated with longer median OS (approximately 25 vs. 20 months; P = 0.003; adjusted OS HR = 0.61), as was higher tumor-bed field intensity ($\geq 1.06$ V/cm; approximately 24 vs. 22 months; P = 0.03; adjusted OS HR = 0.69) [30]. We intentionally rounded these thresholds; their two-decimal precision results from dividing a continuous, isotropic, population-averaged dielectric property-based simulation, not from exact physical constants. With these caveats, the study reported a retrospective quantitative dose–outcome association for TTFields, motivating further study of modeled delivery as a potentially modifiable variable rather than establishing a causal dose threshold. These concepts—power-loss-density and field intensity thresholds, with typical GBM field strengths below 5 V/cm at 200 kHz—have been incorporated into practical planning standards [31]. Whether these thresholds are applicable to extracranial sites remains

uncertain, as they were derived within the brain. An *in vivo* torso study showing field strengths of ≥1 V/cm across the heart, lungs, liver, kidneys, spleen, pancreas, and stomach suggests potential for abdominal coverage but does not provide a site-specific dose–response calibration [32].

## 2.5 Array optimization and delivery interface

Transducer placement primarily controls the shape of the field. Systematic studies of electrode positions reveal that layout optimization can enhance tumor-bed field intensity [33], and personalized configurations have demonstrated improved treatment outcomes in GBM compared to standard placements [34]. Layout-planning tools have been validated for reproducibility [35], and combining finite-element-guided skull modifications with array planning has been shown to enhance dose distribution [36]. Clinical systems typically operate two orthogonal transducer pairs, switching at around 1 Hz, allowing the field to sample multiple directions across cells with varying spindle orientations. The main limitation on achievable intensity is skin heating rather than field strength, as array temperature and specific absorption rate at the scalp or torso set a thermal limit. Additionally, the electrode-skin interface, hydrogel, and skin conductivity influence both dose and heat transfer [37]. The goal of approximately 18 hours of device use daily presents engineering, tolerability, and behavioral challenges.

Current delivery research aims to maximize tumor exposure within safe thermal limits. A computational study optimized multidirectional excitation by allocating time to each direction, focusing energy on lung lesions [38]. Pulsed TTFields employ a lower duty cycle to boost instantaneous field intensity; studies with glioma cells, gel models, and realistic head models demonstrated stronger inhibition with controlled temperature increases [39]. These investigations consider waveform, direction, exposure time, and temperature as interconnected design variables. However, they are still preclinical or based on models and do not replace clinical evidence for continuous-wave wearable systems (Figure 2).

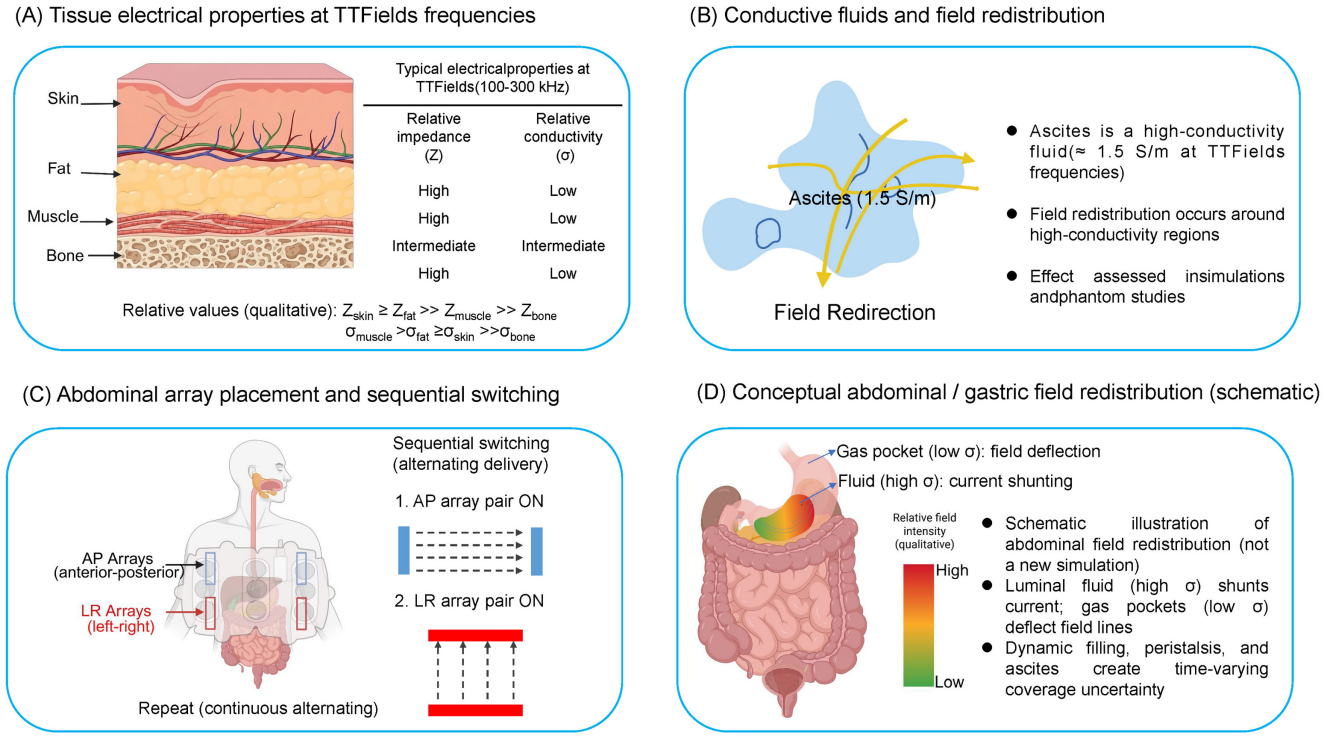



**Figure 2:** Macroscopic field distribution and modulation by body fluids. (A) A qualitative comparison of tissue electrical properties at TTFields frequencies (100–300 kHz) shows the relative impedance and conductivity of skin, fat, muscle, and bone. (B) Conductive body fluids like ascites influence electric-field line redistribution, making them important for simulation and phantom dosimetry. (C) Abdominal array placement is illustrated along with sequential switching between anterior–posterior (AP) and left–right (LR) array pairs. (D) Conceptual schematic of abdominal and gastric electric-field redistribution, illustrating how high-conductivity luminal fluid (current shunting), low-conductivity gas pockets (field-line deflection), and time-varying gastric geometry create spatial and temporal dose uncertainty across the gastric wall. Panels (B) and (D) are qualitative conceptual illustrations rather than patient-specific numerical simulations or direct *in vivo* measurements.

**Table 2:** Key multiscale bioelectric and mechanical parameters

| Scale | Effect/target | Frequency | Intensity/threshold | Readout | System | Maturity | References |
|---|---|---|---|---|---|---|---|
| Macro | Field distribution and dose-survival | 200 kHz, GBM | LMiDD ~0.77 mW/cm³; ~1.06 V/cm, simulation cut points | OS/PFS association | EF-14 simulation, n=340 | L1–L2 | [30] |
| Macro | Body-fluid modulation | 100–300 kHz | Conductivity dependent | FEM field maps | Head and torso models | L2 | [28, 29] |
| Macro | Extracranial lung coverage | 150 kHz | ≥1 V/cm coverage threshold | FEM maps and experimental bridge | Duke/Ella lung models | L1–L2 | [25, 38] |
| Delivery | Multidirectional or pulsed optimization | 150–200 kHz | Instantaneous intensity, energy distribution, and temperature rise | Coverage, cell viability and thermal safety | Lung model, glioma cells, gel and head models | L1 | [38, 39] |
| Meso | Microtubule/septin dielectrophoresis | 150–200 kHz | Clinical, 1–3 V/cm | Spindle disruption and mitotic catastrophe | Cell lines and molecular dynamics | L1 | [42, 43, 45] |
| Meso | Nanomechanical remodelling | 150 kHz | Clinical | AFM stiffness and elasticity | PDAC plus ECM co-culture | L1 | [51] |
| Meso | Migration and invasion | 200 kHz 150 kHz | GBM invasion, 0.6 V/cm RMS; migration, 1.75 V/cm RMS. Migration/invasion, 0.9 V/cm | GEF-H1/RhoA/ROCK and motility | GBM cells | L1–L2 | [59, 60] |

Footnote: Values are assay-specific. RMS denotes root mean square; the convention is retained only where explicitly reported in the source.

### 2.6 Boundaries of the macroscopic perspective

The macroscopic model is the most advanced stage on the scale ladder, but it relies on assumptions that should be approached with caution. Most simulations assume tissue to be isotropic and use average dielectric properties for populations, yet real tissues are anisotropic and vary between patients. For example, in pancreatic cancer, practical limits to efficacy with alternating fields are partly due to attenuation and delivery challenges, demonstrating that having a sufficiently accurate computed field is necessary but not enough for a biological effect [40]. The skin presents a particular bottleneck because its dielectric properties significantly influence how much field reaches the torso [41]. Within our revised framework, macroscopic field modeling in phantoms and anatomic simulations is supported at L1–L2, whereas the retrospective LMiDD–survival association in the EF-14 glioblastoma cohort represents an exploratory clinical dose–outcome correlation rather than an L3 causal bridge, because LMiDD incorporates device-use adherence and lacks independent multi-cohort validation or extracranial calibration. A summary of representative multiscale physical and mechanical parameters and their maturity levels is provided in Table 2.

## 3. Nanomechanical feedback: the mechanical interaction between the field and the cytoskeleton

If the macroscopic fingerprint is a field map, then the mesoscale fingerprint is mechanical: it involves the forces exerted by the field on the cell's most polar structures and the resulting changes in mechanical phenotype. This level links the physics of TTFields with mitosis biology and is where the primary mechanism—dielectrophoretic interference with the spindle—has been most clearly studied.

### 3.1 Dielectrophoretic effect on microtubules and septins

The core theory suggests that intermediate-frequency fields influence tubulin dimers, which have substantial dipole moments, and septin filaments that shape the cleavage furrow. Live-cell experiments demonstrated that these fields slow down and reduce microtubule growth during spindle formation, resulting in faulty chromosome separation and mitotic failure [42]. An alternative mechanism was found for septins; when they detach from the spindle midline and cleavage furrow, it causes abnormal mitotic exit and membrane blebbing [43]. The biophysical plausibility of these effects has been quantified: estimates of the forces and torques acting on tubulin, microtubules, and septins by the field have been calculated [44], and molecular-dynamics simulations reveal that the tubulin dipole reorients depending on field direction [45]. An illustrative energy estimate highlights the challenge. Taking the representative free-tubulin-dimer dipole moment of 3000 D used by Tuszynski *et al*. (approximately $1.00 \times 10^{-26}$ C· m) [44], and a reference field magnitude E = 2 V/cm = 200 V/m, gives pE ≈ $2.00 \times 10^{-24}$ J. At 310 K, kBT ≈ $4.28 \times 10^{-21}$ J; thus pE/kBT ≈ $4.7 \times 10^{-4}$, or approximately 1/2100. In this simple dipole model, the interaction-energy scale is too small to make stable single-dimer alignment against thermal fluctuations likely; the estimate does not establish the net response to an alternating field. Instead, the proposed mechanism relies on two amplification effects: cooperativity, where a growing microtubule comprises hundreds to thousands of partially aligned dimers, increasing their collective interaction with the field; and field intensification at the cleavage furrow, where narrowing during cytokinesis concentrates current and enhances the local field, leading to stronger

dielectrophoretic forces proportional to $\nabla|E|^2$. Both effects are physically plausible, but neither has been directly measured in dividing cells, and thus the connection between field exposure and spindle disruption remains predictive rather than experimentally confirmed.

This unresolved gap explains why a recent electrodynamic study is significant: it suggests that the direct force exerted on microtubules at clinical field strengths could be weaker than generally believed, indicating that some of the antimitotic effects might be indirect [46]. Considering the energy budget of a single dimer mentioned earlier, this is not a minor point but a genuine alternative; if the cooperative and furrow-intensification mechanisms are smaller than estimated, then the core idea of 'bioelectric–mechanical coupling' discussed in this review is not fully supported at its most basic level. Consequently, we rate the direct-dielectrophoretic mechanism at L1 rather than L2 (see Box 1), and view the mechanical scale as the most uncertain aspect of the framework, not its most well-founded.

### 3.2 Measuring single-cell nanomechanics using atomic force microscopy

Independent of TTFields, the mechanical phenotype of cancer cells now serves as a measurable biomarker. Atomic force microscopy revealed that metastatic cancer cells from patient body fluids are over 70% softer than benign cells, with a narrower range of stiffness, indicating cell softening as a malignancy marker [47]. Indentation-type atomic force microscopy (AFM) on unprocessed human biopsies identified a clear low-stiffness peak associated with breast-cancer progression [48], while more advanced methods like real-time deformability cytometry enable label-free mechanical phenotyping that detects changes in the cytoskeleton [49]; these techniques are increasingly used for diagnosis and treatment monitoring [50]. Notably, the strongest evidence that TTFields modify the mechanical phenotype comes from pancreatic ductal adenocarcinoma cells grown with extracellular matrix, where field exposure changed the nanomechanical properties of both the cells and their surrounding matrix [51]. This single-cell measurement currently stands as one of the few links between TTFields exposure and a quantitative mechanical change, though it needs validation across different tumor types.

### 3.3 Axes of mechanotransduction connecting stiffness with signaling pathways

Changes in the cytoskeleton and cell stiffness are not just mechanical; they activate specific mechanotransduction pathways. The YAP/TAZ pathway is the main route, translating tension within the cytoskeleton and matrix stiffness into changes in gene expression [52]. This function is part of the broader roles of Hippo signaling and mechanical cues [53], and it is directly linked to tumor initiation, stem cell properties, and resistance to chemotherapy [54]. Matrix mechanics influence this system via integrin clustering and focal adhesion signals [55, 56], while mechanosensitive channels like Piezo1 convert stiffness signals into $Ca^{2+}$/calpain/YAP activity, contributing to disease progression [57]. For TTFields, disrupting the cytoskeleton may hinder not only cell division but also impair this mechanotransduction pathway, supported by evidence that cytoskeletal remodeling affects cancer severity through related signaling [58]. However, a major challenge arises: the YAP/TAZ–integrin–Piezo1 pathway responds to mechanical cues over seconds to hours, but TTFields operate at a frequency of 100–300 kHz, producing effects only during the brief mitotic phase. How such a high-frequency field can induce sustained cytoskeletal tension necessary for nuclear YAP movement remains unclear in current studies. This frequency and timescale mismatch is, in our view, the main unresolved issue concerning this pathway. Thus, the connection for TTFields is still hypothetical, as indicated in Figure 3.

### 3.4 Migration, invasion, and electrotaxis

The mechanical effects of TTFields also influence motility. The most comprehensive mechanistic study indicates that TTFields hinder cancer-cell migration and invasion by disrupting microtubule and actin dynamics and activating the GEF-H1/RhoA/ROCK pathway [59]. Consistent reductions in migration, invasion, and angiogenesis have been observed in glioblastoma [60], along with a reversal of mesenchymal (epithelial-to-mesenchymal transition) markers [61]. Additionally, the broader concept of electrically guided motility, galvanotaxis, offers supporting evidence: direct-current fields can modulate cancer-cell movement depending on confinement [62], and the mechanical tumor microenvironment interacts with migration via Rho/ROCK-mediated cytoskeletal remodeling [63]. Early *in vivo* studies have shown that alternating fields can inhibit metastatic spread in animal models [64]. Collectively, these findings imply that TTFields not only limit proliferation but also interfere with the mechanical processes involved in tumor dissemination, although the clinical relevance of its anti-migratory effects remains to be fully established.

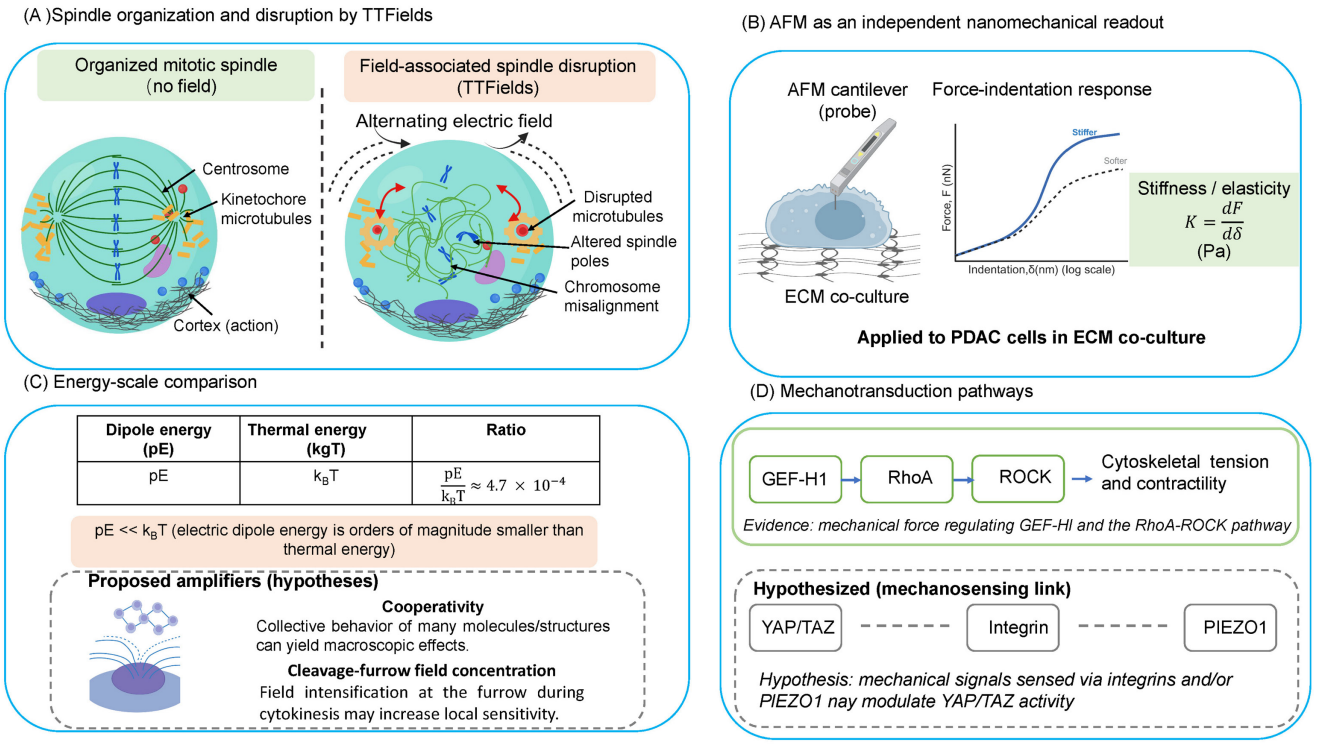



**Figure 3:** Alternating fields and cellular nanomechanics. (A) A schematic contrasts organized mitotic spindle architecture without the influence of fields and the disruption caused by TTFields. (B) AFM serves as an independent nanomechanical measurement method, showing force–indentation analysis in ECM co-culture systems. (C) The energy-scale comparison highlights that electric dipole energy (pE) is significantly lower than thermal energy (kBT), with proposed amplifiers or hypotheses for cooperativity and cleavage-furrow field concentration. (D) Mechanotransduction pathways are divided into a supported direct pathway (GEF-H1–RhoA–ROCK) and a hypothesized mechanosensing link involving YAP/TAZ, integrin, and PIEZO1, with solid and dashed lines indicating supported versus hypothesized relationships.

According to the grading scheme, the nanomechanical rung is positioned at L1: a mechanical readout has been observed in at least one tumor type [51], and its frequency dependence is noted. However, the direct-force mechanism is not fully established (see Box 3), and the only TTFields-specific nanomechanical dataset remains unreplicated. Moreover, the connection between changes in nanomechanics and clinical outcomes is still associative rather than causal. This represents the weakest level in the framework, and we highlight this rather than assuming clinical success of the modality creates confidence.

## 4. Microscale multi-omic fingerprints: enabling real-time monitoring of single-cell responses

The molecular response to TTFields is dynamic, and endpoint assays that require cell lysis only capture its final state. Consequently, the fingerprint at this scale is a time-resolved molecular signature in living single cells, including metabolic, transcriptomic, membrane-biophysical, and immunological aspects. The key advancement has been the development of platforms capable of reading this signature without destroying the cell.

### 4.1 Performing single-cell multi-omics analysis on a chip

A new generation of microchip platforms enables the tracking of multiple molecular species within the same living cell over time. Spatial-temporal multi-omic profiling of live single cells on a chip has been demonstrated, particularly in cancer therapy, allowing researchers to observe molecular responses over a trajectory instead of a single snapshot [65]. The core toolkit combines dielectrophoretic or micropillar-array capture methods with surface-enhanced Raman spectroscopy (SERS): single-cell on-chip SERS quantifies metabolites like pyruvate, ATP, and lactate [66]; SlipChip-SERS identifies single-cell metabolic fingerprints [67]; micropillar arrays isolate rare cells for subsequent single-cell proteomics [68]; and dielectrophoresis-based SERS sensors integrate bioelectric manipulation with molecular detection [69]. Recent reviews have highlighted the maturation of single-cell SERS as a tool to resolve cellular heterogeneity [70]. Concerning TTFields, these platforms are relevant because they can monitor the molecular effects of the field in real time, and many use electric fields for cell handling, creating a direct connection between measurement technology and therapy.

### 4.2 Metabolic reprogramming and energy dynamics

Cancer metabolism offers a key insight into the field's impact. The Warburg phenotype, characterized by aerobic glycolysis that promotes proliferation, explains why metabolic monitoring is valuable [71]. Label-free optical techniques like NAD(P)H/FAD redox imaging connect a cell's glycolytic state to how it responds to treatment [72], while stimulated-Raman-scattering imaging observes lipid metabolism in living cells under stress [73]. High-throughput single-cell metabolomics now allows for the analysis of metabolic heterogeneity within a treated cell population [74]. Real-time, on-chip tracking of cancer cells after TTFields exposure reveals spatial and temporal changes in metabolic signatures, suggesting reduced glycolysis [65]. However, this finding is based on a single-platform study, and the direct link between field exposure and specific metabolic changes at the single-cell level needs further validation and independent replication.

### 4.3 Transcriptomic signature and genomic instability

At the transcriptional level, TTFields exhibit a signature consistent across various tumor types, as identified by a multi-cancer analysis. This signature includes the downregulation of cell-cycle and DNA-repair pathways and the upregulation of stress responses such as autophagy, apoptosis, and senescence [75]. This commonality across cancers suggests a shared underlying mechanism rather than tumor-specific differences, and it supports the resistance circuitry discussed in Section 5. However, this conclusion is based on a single study, and an alternative interpretation remains possible: any strong mitotic arrest could produce a similar pattern of reduced cell-cycle activity and increased stress responses. Therefore, the signature might reflect an endpoint of cell division arrest rather than a TTFields-specific causal program. Differentiating these possibilities requires comparison with other antimitotic agents, which has not yet been conducted.

### 4.4 Membrane biophysical properties

The cell membrane functions both as a target and a sensor. TTFields enhances membrane permeability in glioblastoma cells, as shown by increased entry of membrane-associated agents like Dextran-FITC and improved uptake of chemotherapeutic drugs, suggesting the formation of reversible nanoscale pores [76]. Differences in membrane fluidity between normal and cancer cells serve as a biophysical marker important for diagnosis and therapy [77], and real-time SERS can track membrane-related microenvironmental factors such as extracellular pH during apoptosis [78]. These membrane alterations link to the delivery and sensitization methods discussed in Section 6, where similar permeability is therapeutically exploited.

### 4.5 Immunogenic cell death and activation of the innate immune system

The most significant molecular marker may be immunological. TTFields causes immunogenic cell death, releasing key damage-associated molecular patterns like calreticulin, HMGB1, and ATP, which are identified using established criteria [79-81]. In preclinical studies, this form of immunogenic death improved anti-tumor effects when used with anti-PD-1 therapy [82]. A specific innate immune mechanism has been identified: TTFields produces micronuclei and cytosolic double-stranded DNA that activate both the STING and AIM2 inflammasome pathways, promoting adjuvant immunity in glioblastoma [83]. Similar immunogenic signatures have been observed in other cancers, including biliary tract cancer cell lines [84]. This immunological signature provides the strongest current rationale for combining TTFields with immunotherapy (Section 6), though it remains unclear whether immunogenic cell death directly drives clinical benefit or is simply a secondary effect of mitotic disruption.

According to the grading scheme, the multi-omic level is at L1: it offers detailed descriptions and is becoming more real-time, yet the causal link from a single-cell molecular change to the tumor-level response is still in development (Figure 4) (Table 3).

## 5. Rewiring signaling circuits and addressing systemic resistance

Sustained field stress does not make the cell's signaling architecture fixed. Instead, it causes adaptive rewiring: the survival circuits that cancer cells activate to withstand ongoing mitotic interference, which both weaken the response and identify targets for sensitization.

### 5.1 Remodeling of stress-signaling networks adaptively

TTFields activate multiple stress-response networks rather than targeting a single pathway. In glioblastoma, applying TTFields reduces migration and invasion by coordinating changes in NF-κB, MAPK, and PI3K/AKT signaling [60], pathways that are well recognized as therapeutic targets [85]. The transcriptomic profile described in Section 4, showing decreased cell-cycle and DNA-repair activity alongside increased stress responses, reflects this molecular reprogramming [75]. Overall, this suggests

that cells do not simply die when mitotic processes are disrupted but instead actively alter their signaling pathways to survive.

### 5.2 Activation of PI3K/AKT bypass

A key focus in this adaptation is PI3K/AKT/mTOR. Research on how cells respond to TTFields indicates that PI3K/AKT signaling plays a role in survival mechanisms and resistance [86], aligning with its known function as a central point for adaptive bypass and resistance to targeted therapies across various cancers [87]. Mechanical disruption of the cytoskeleton (see Section 3) may also activate this pathway via mechanotransduction, offering a way for physical stimuli to influence this primary survival pathway. Although this connection is mechanistically plausible, it has not yet been directly proven.

### 5.3 Autophagy and endoplasmic reticulum stress as cellular survival mechanisms

Autophagy is one of the most well-supported survival mechanisms. When exposed to TTFields, AMPK-dependent autophagy increases and acts protectively, as reducing AMPK or ATG7 levels, or inhibiting with chloroquine, makes cells more vulnerable to the field [88]. This highlights autophagy's typical, context-dependent dual role in cancer therapy [89]. Additionally, the aneuploid offspring of faulty mitosis experience heightened endoplasmic-reticulum stress, activating the unfolded protein response [90], which also links to antitumor immunity [91]. These responses are adaptive rather than permanent, and targeting them pharmacologically is a logical way to increase sensitivity.

### 5.4 Targeting the rewired circuit for sensitization

Adaptive resistance can be countered by blocking escape routes, which enhances the treatment effect. For example, inhibiting the mitotic checkpoint increases TTFields-induced G2/M arrest and apoptosis [92], and kinase inhibitors can serve as sensitizers, as demonstrated by sorafenib in glioblastoma [93]. Another promising approach targets induced DNA-repair deficiencies: TTFields causes homologous-recombination deficiency in ovarian cancer cells, reducing drug resistance and justifying combination with PARP inhibitors [94]. Preclinical studies also support combining TTFields with sorafenib in hepatocellular and colorectal cancer models [95, 96, 97]. The reported mechanisms depend on the model; AKT/STAT3 inhibition was demonstrated in the colorectal-cancer study [96]. These strategies link the resistance mechanisms discussed here to the physico-chemical sensitization approaches described in Section 6.

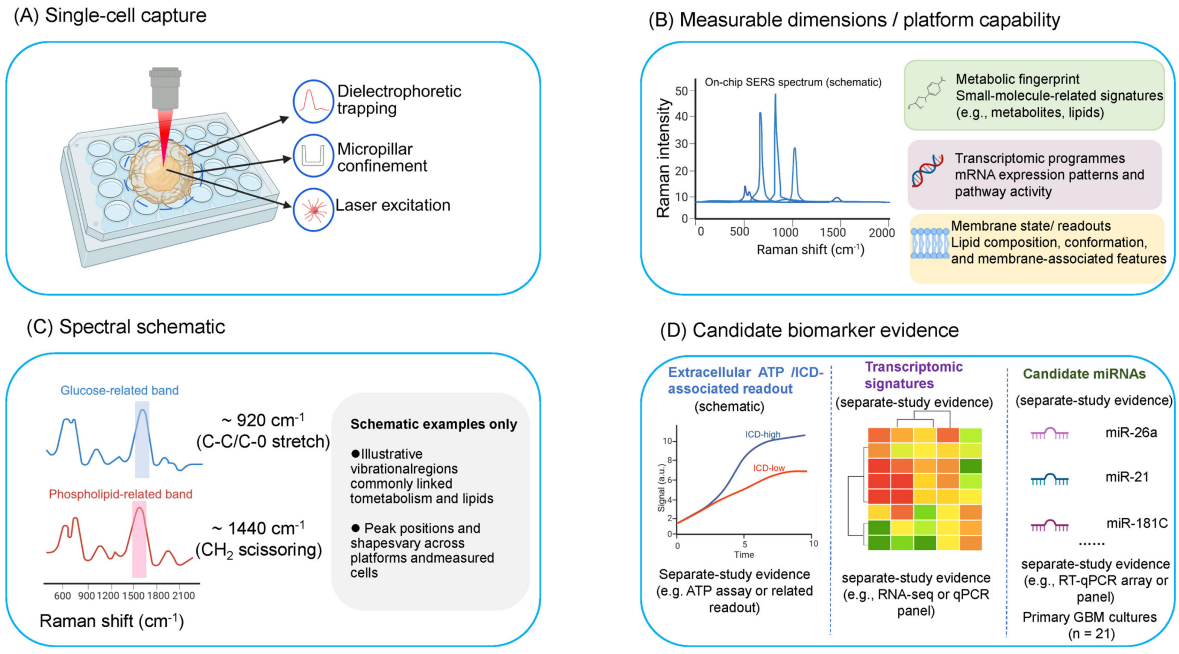



**Figure 4:** Workflow for Single-Cell SERS and Multi-Modal Measurement. (A) An illustration of the single-cell capture process, encompassing dielectrophoretic trapping, micropillar confinement, and laser excitation for analysis on a chip. (B) A summary of platform capabilities across measurable dimensions, including a schematic SERS spectrum and three primary categories of readouts: metabolic fingerprints, transcriptomic profiles, and membrane-state metrics. (C) Spectral examples are explicitly schematic, emphasizing representative bands related to glucose and phospholipids without suggesting a specific original dataset. (D) Candidate biomarker evidence is presented in three separate blocks: extracellular ATP/ICD-associated readouts, transcriptomic signatures, and candidate miRNAs. These findings originate from separate studies, not a single platform, experiment, or common cohort. The primary-GBM culture descriptor (n = 21) applies only to the candidate-miRNA study [120]. This figure delineates platform capability, schematic spectral interpretation, and candidate biomarker evidence derived from separate studies.

**Table 3:** Reported TTFields-associated molecular responses and candidate measurement platforms (representative)

| Omic layer | Marker/signature | Direction | Platform | Cancer type | References |
|---|---|---|---|---|---|
| Metabolic response | Glucose, pyruvate, ATP and lactate during TTFields plus sorafenib | Time- and treatment-dependent; not attributable to TTFields alone | Living single-cell multi-omic chip | Huh7 hepatocellular carcinoma cells | [65] |
| Candidate metabolic measurement platforms | Pyruvate/ATP/lactate or NAD(P)H/FAD redox state | N/A (platform capability; not a TTFields response) | Single-cell SERS / optical redox imaging | Multiple cancer models | [66, 72] |
| Transcriptomic | Cell-cycle and DNA-repair genes | Decreased | Bulk/multi-cancer RNA | Pan-cancer | [75] |
| Transcriptomic | Stress programs (autophagy/apoptosis/senescence) | Increased | Bulk/multi-cancer RNA | Pan-cancer | [75] |
| Membrane | Permeability (Dextran-FITC ingress) | Increased, reversible | Bioluminescence/dye uptake | GBM | [76, 98] |
| Immunogenic | Calreticulin / HMGB1 / ATP (DAMPs) | Increased | ICD consensus assays | Multiple; biliary | [82, 84] |
| Innate immune | STING / AIM2 inflammasome (micronuclear dsDNA) | Activated | Pathway assays | GBM | [83] |

According to the grading scheme, the resistance rung is classified as L2 for the autophagy and checkpoint mechanisms, based on *in vitro* functional validation. However, it remains at L1 regarding the translation of these mechanisms into clinically observed resistance, which is mostly inferred rather than directly measured in patients (Figure 5).

## 6. Synergistic sensitization: physical and chemical interactions across physiological barriers

The therapeutic benefit of TTFields is growing, mainly through its capacity to enhance other agents' effects. Combination strategies draw on several distinct processes, including membrane or barrier modulation, impaired DNA repair, and immune activation. The following sections distinguish their supporting evidence rather than attributing all combinations to a single sensitization mechanism (Table 4).

### 6.1 Membrane permeabilization and drug delivery

The membrane-permeability effects covered in Section 4 can enhance intracellular drug exposure during co-administration. Reviews have explored the biophysics behind field-mediated membrane permeabilization in cancer [12]. More recent studies show that TTFields-induced permeability depends on the G2–M phase, is reversible, and selectively affects cancer cells, offering a potential way to improve chemotherapy uptake and combat multidrug resistance [98]. Standardized assays are now available to measure this effect [99]. Although the permeability window could be scheduled, its timing and strength need to be determined experimentally for each specific combination.

TTFields must be clearly distinguished from other electric-field-assisted delivery methods. A recent review on non-superficial tumor drug delivery outlined techniques such as electromigration, electro-osmosis, electroporation, TTFields-related permeability changes, and electrostatic deposition of intraperitoneal aerosols [100]. While all these methods utilize an external electric field to influence transport, their field strengths, durations, and tissue impacts vary. For example, electrochemotherapy and irreversible electroporation depend on high-field membrane disruption or ablation. In contrast, TTFields operate at lower intensities and intermediate frequencies over much longer durations. Consequently, although alternative modalities in gastric and abdominal tumors raise questions about barriers and drug distribution, their efficacy and safety are not directly applicable to TTFields.

### 6.2 Regulation of the blood–brain barrier

TTFields have been investigated as a means of transiently increasing blood‐brain barrier (BBB) permeability. In preclinical models, BBB permeabilization was associated with Rho-kinase-mediated claudin-5 phosphorylation, and combining TTFields with paclitaxel reduced tumor volume in glioma-bearing rats [101]. A human-derived three-dimensional *in vitro* BBB model also showed junctional alterations and increased permeability, with barrier integrity recovering 48 h after TTFields cessation [102]. An exploratory retrospective perfusion-MRI study in patients with glioblastoma reported increased permeability-related measures and relative cerebral blood volume with TTFields plus temozolomide compared with temozolomide alone [103]. These imaging observations do not establish improved drug delivery or clinical benefit.

The findings provide a rationale for studying transient barrier modulation in the central nervous system (CNS). However, the cerebral endothelial barrier differs from abdominal and thoracic barriers. BBB-specific findings cannot be assumed to apply to gastric, pancreatic, or other extracranial tumors without site-specific validation.

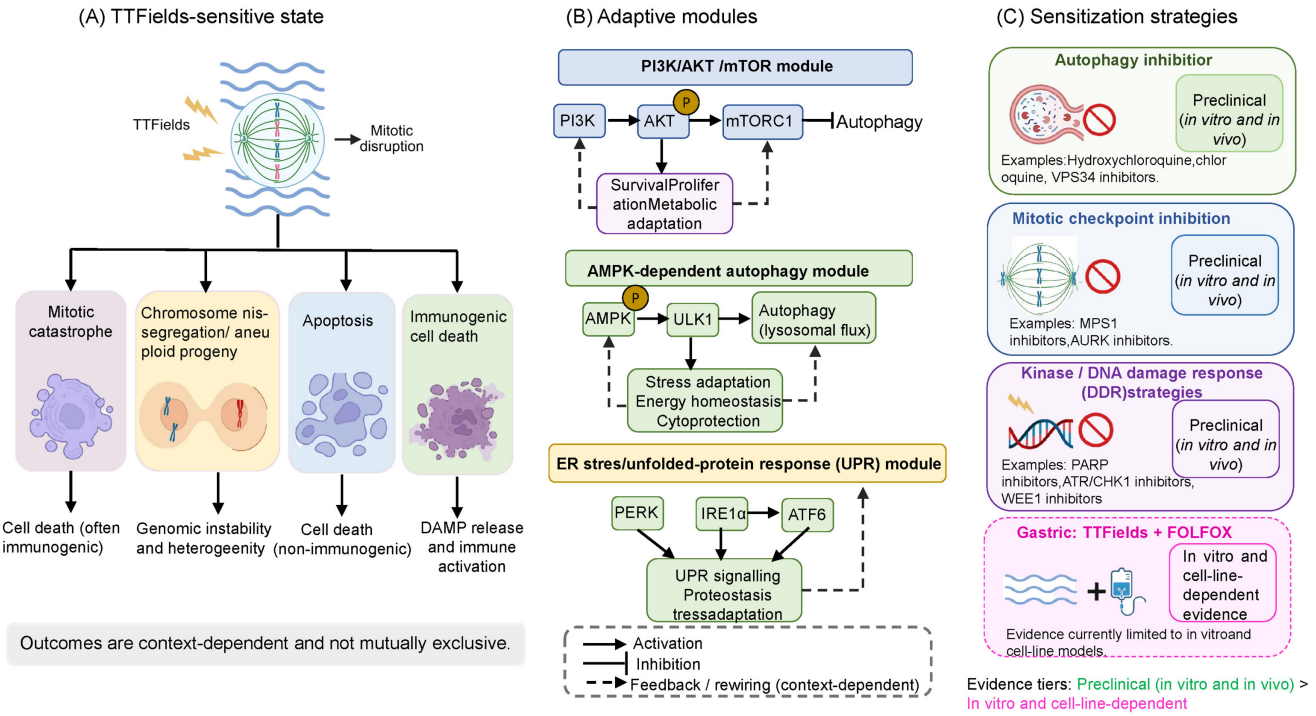



**Figure 5:** Signaling Rewiring from a Sensitive to a Field-Tolerant State. (A) TTFields-sensitive states are associated with multiple context-dependent outcomes, including mitotic catastrophe, chromosome mis-segregation/aneuploid progeny, apoptosis, and immunogenic cell death; these pathways are not mutually exclusive and should not be interpreted as a single obligatory linear cascade. (B) Adaptive modules potentially linked to field tolerance encompass PI3K/AKT/mTOR signaling, AMPK-dependent autophagy, and endoplasmic reticulum (ER) stress / unfolded-protein response (UPR) pathways. (C) Sensitization strategies are categorized by evidence tier, including autophagy inhibition, mitotic checkpoint inhibition, and kinase / DNA damage response strategies supported preclinically. Meanwhile, gastric TTFields combined with FOLFOX are presented separately, based on *in vitro* and cell line-dependent evidence. Activation, inhibition, and feedback/rewiring that depend on the context are indicated by different line styles.

**Table 4:** Representative TTFields combination and sensitization strategies

| Partner modality | Mechanism | Model | Effect | Stage | References |
|---|---|---|---|---|---|
| Gemcitabine/nab-paclitaxel | Clinical combination; specific mechanistic contribution not established by the trial | Locally advanced pancreatic adenocarcinoma | Median OS 16.2 vs 14.2 months | Randomized phase 3 (PANOVA-3) | [8] |
| Chemotherapy or taxanes | Microtubule overlap and/or permeability | Preclinical NSCLC and related models | Improved efficacy in experimental models | Preclinical | [106, 112] |
| FOLFOX | DNA-repair or FA-BRCA downregulation and sensitization | AGS and KATO III gastric-cancer cells | Lower cell count and clonogenic growth; interaction differs by cell line | Preclinical *in vitro* | [9] |
| Radiotherapy | Delayed double-strand-break repair and induced BRCAness | GBM and NSCLC | Radiosensitisation | Preclinical | [104, 105] |
| Concurrent chemoradiotherapy implementation | Convergent DNA damage and array-dose interface | GBM and phantom | No significant PFS/OS difference in a real-world cohort; array alters surface and depth dose | Real-world plus physical dosimetry | [109-111] |
| DDR inhibitors (PARP or ATR) | Exploits induced homologous recombination deficiency | Glioma stem-like and ovarian models | Reduced clonogenic survival | Preclinical | [94, 108] |
| Immune checkpoint (anti-PD-1 or anti-PD-L1) | Immunogenic cell death and chemokine-mediated T-cell infiltration | NSCLC *in vivo* | Enhanced response in models; patient benefit unproven | Preclinical; clinical benefit unproven | [82, 115, 116] |
| Sorafenib | Model-dependent sensitization; AKT/STAT3 inhibition reported in colorectal models | HCC and colorectal models | Reduced proliferation | Preclinical | [95-97] |
| Mild hyperthermia or ZnO nanoparticles | Additional cytotoxicity | Pancreatic and other models | Enhanced apoptosis | Preclinical | [113, 114] |
| BBB modulation | Reversible claudin-5 relocalisation | *In vitro*, *in vivo* and human imaging | Potentially improved CNS drug delivery | Preclinical plus human imaging | [101, 103] |

## 6.3 Interaction between radiotherapy and chemotherapy

TTFields and cytotoxic therapy intersect on DNA-damage pathways by delaying repair post-irradiation and increasing chromatid aberrations [104]. In NSCLC, reduced BRCA1 signaling and impaired double-strand-break repair create a vulnerability to radiation, often termed "BRCAness" [105]. Alternating fields also enhance chemotherapy

effectiveness in NSCLC models, with an optimal frequency around 150 kHz [106]. In glioblastoma cell lines, TTFields boost the impact of temozolomide and lomustine by downregulating the Fanconi anaemia/BRCA pathway [107]. Combining TTFields with PARP1 or ATR inhibitors further diminishes clonogenic survival in glioma stem-like cells [108].

Evidence for gastric cancer directly involves the same DNA-damage and chemotherapy pathways. In AGS and KATO III cells, exposure to 150 kHz TTFields reduced cell counts to about 53% and 57% of control, respectively. After 72 hours, their clonogenic capacity dropped to roughly 62% and 41% of control levels. Combining cell count and clonogenic capacity as the composite overall-effect measure yielded values of approximately 37% and 24% of control for AGS and KATO III cells, respectively. FOLFOX treatment further decreased viable cell fractions beyond either treatment alone. The interaction was described as additive, with a slight tendency toward synergy in AGS cells and toward antagonism in KATO III cells. Transcriptomic and protein analyses showed impaired DNA repair, notably downregulation of the FA-BRCA pathway [9]. This offers a direct, measurable starting point for testing TTFields combined with standard gastric cancer chemotherapy, but it requires independent validation and remains an *in vitro* study. No gastric cancer animal models, patient-specific abdominal field calibration, or survival endpoints have been reported (Table 5).

Introducing clinical implementation of radiotherapy presents a distinct physical challenge. A multicenter real-world study of 100 newly diagnosed GBM patients who received TTFields alongside chemoradiotherapy, then either continued or discontinued during adjuvant temozolomide, found median PFS of 12.8 versus 12.5 months and median OS of 20.6 versus 16.6 months; neither difference was statistically significant. The median usage was about 20 hours daily, with grade 3 scalp toxicity in roughly 3% of patients [109]. These findings support the feasibility of the approach but do not confirm that all combinations are synergistic. The arrays also interfere with radiation doses. In a solid-water phantom, a 3 × 3 Optune ceramic array decreased the 6-MV photon dose by around 2–4% at a depth of 10 cm and significantly increased dose at the surface. MOSFET and diode measurements were approximately 1.81–1.87 times the baseline without the array; film measurements were higher and influenced by energy response. Repositioning the array reduced peak surface dose by up to 40%, although hotspots persisted and residual surface dose was about 1.6–2.3 times baseline [110]. Therefore, TTFields-radiotherapy combinations demand careful treatment planning, array positioning, and skin-dose management alongside a molecular rationale [111].

### 6.4 Anti-microtubule agents, nanomaterials, hyperthermia, and immunotherapy

The overlap between microtubule-targeting drugs and taxanes makes taxanes a logical partner, with the rationale for their combined use well established [112]. Several other physical and chemical methods have also shown promise in preclinical studies: zinc-oxide nanoparticles can boost apoptosis and genotoxicity when used with TTFields [113], and mild hyperthermia has been identified as a supportive treatment that enhances the effectiveness of TTFields in pancreatic cancer [114]. The immune-related features discussed in Section 4 support combining TTFields with checkpoint inhibitors. In NSCLC models, this combination is effective *in vivo*, partly due to increased chemokine expression—such as CCL2/8 and CXCL9/10—that aids T-cell infiltration and improves anti-PD therapy [115, 116]. Collectively, these insights and the longstanding evidence that combining different modalities improves outcomes [117] position sensitization as a highly feasible clinical strategy within the cross-scale framework.

Within the mechanistic grading scheme (L0–L3), sensitization mechanisms are heterogeneous. Membrane-permeability and DNA-repair-related sensitization are supported at L1–L2 in preclinical models, and blood–brain barrier modulation is supported at L1–L2 preclinically with exploratory human imaging observability, without demonstrating an L3 cross-scale predictive bridge in an independent dataset. Immunotherapy and nanomaterial combinations remain at preclinical L1, with clinical efficacy tracked separately on the clinical evidence axis. These separate pathways involving membranes, the blood-brain barrier, and combinations are summarized in Figure 6.

## 7. Future directions: progressing based on evidence maturity

Future directions can be grouped into six development stages: field-dose verification, extraction of biological-effect features, endpoint definition, analytical validation, clinical validation, and adoption through regulations or guidelines. Field-dose verification includes measurements and simulations. Biological features include mitotic indices and immunogenic markers; clinical endpoints include OS, PFS, and adherence thresholds. The diagram outlines development tasks, not a strict sequence. Results may lead to adjustments to parameters, readouts, or endpoints (Figure 7).

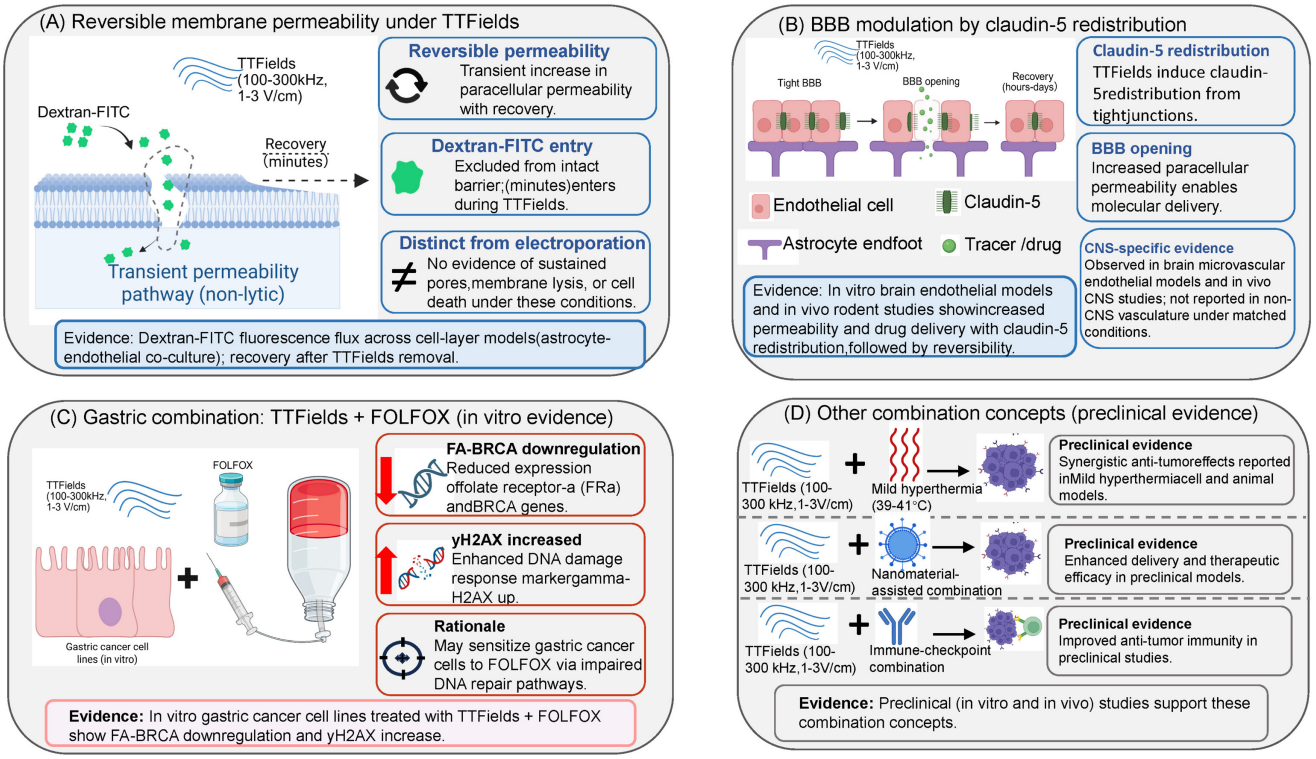



**Figure 6:** Barrier remodeling and physicochemical combinations. (A) TTFields-associated membrane permeability is depicted as a reversible, transient, non-lytic permeability pathway that permits dextran-FITC entry and recovers after field removal, and is explicitly distinguished from electroporation. (B) Modulation of the BBB is illustrated as claudin-5 redistribution, transient BBB opening, and recovery, with particular emphasis on the CNS-specific nature of the supporting evidence. (C) A gastric-combination panel summarizes *in vitro* evidence for TTFields in conjunction with FOLFOX, including FA–BRCA downregulation, increased γH2AX, and a proposed rationale related to impaired DNA-repair capacity. (D) Additional combination strategies, including mild hyperthermia, nanomaterial-assisted combinations, and immune-checkpoint strategies, are presented as preclinical evidence. Evidence footnotes are retained to distinguish barrier-remodeling findings from broader combination approaches.

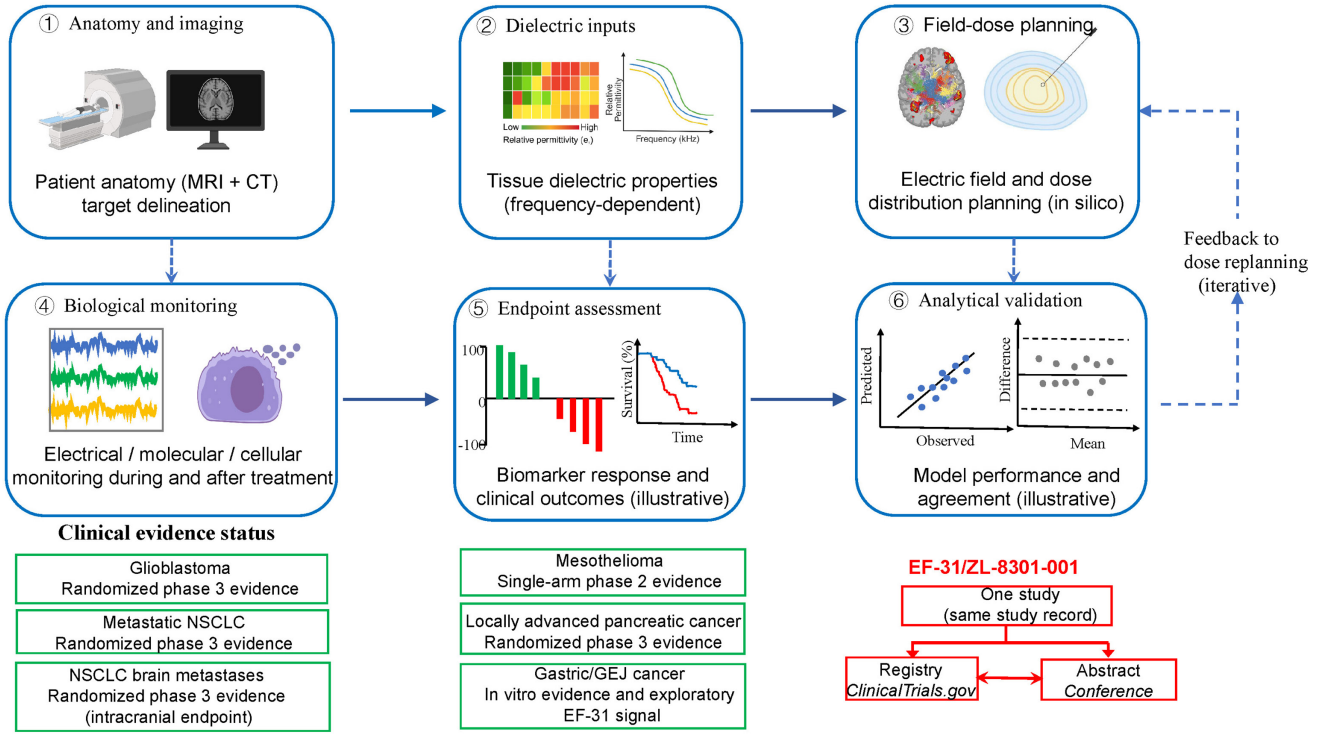



**Figure 7:** The precision bioelectronics pipeline and clinical evidence status. It shows a six-step workflow starting from anatomy/imaging and dielectric inputs, moving through field–dose planning, biological monitoring, endpoint assessment, and analytical validation. The dashed feedback loop highlights that dose planning is iterative rather than strictly linear. The schematic panels for endpoint assessment and validation are illustrative. The bottom section summarizes study-design categories by indication, rather than assigning mechanistic L0–L3 grades from trial phase. Gastric/GEJ cancer remains exploratory. EF-31/ZL-8301-001 is shown as one study with registry and abstract records, not independent replications.

**Table 5:** Evidence for TTFields and primary gaps in gastric and gastro-oesophageal junction cancer

| Evidence layer | Available evidence | What it supports | What it does not support | Mechanistic maturity (L0–L3)/ clinical status | References |
|---|---|---|---|---|---|
| Peer-reviewed gastric-cancer *in vitro* study | TTFields alone (150 kHz, 72 h): AGS, 1.1 V/cm RMS—cell count 53%, colony-forming ability 62%, composite overall effect 37% of control; KATO III, 1.7 V/cm RMS—cell count 57%, colony-forming ability 41%, composite overall effect 24% of control. FOLFOX further reduced viability; the interaction was additive, with a slight tendency toward synergy in AGS and toward antagonism in KATO III. FA-BRCA and DNA-repair pathways were downregulated | Gastric-cancer cells show a direct measurable response; the FOLFOX combination has a reproducible experimental entry point. | Animal efficacy, patient efficacy, achievable abdominal dose, or consistent synergy across cell lines. | L1 | [9] |
| Exploratory clinical study, two records from the same EF-31 study | NCT04281576/EF-31/ZL-8301-001 was a single-arm, open-label phase II study with 28 enrolled patients and completed status. The registry still reported "No Results Posted" on 24 July 2026. Annals of Oncology LBA3 reported first-line TTFields plus XELOX results from the same study. | Clinical exploration in gastric/GEJ cancer occurred; the registry and abstract provide complementary design and results information. | The two records are not independent replications. An abstract-only, single-arm result cannot establish incremental benefit over XELOX or replace a full peer-reviewed paper and mature safety analysis. | Clinical track: exploratory single-arm phase II signal (mechanistic L0–L3 not applicable) | [10, 11] |
| Abdominal field feasibility inferred from other sites | *In vivo* torso work detected ≥1 V/cm in the stomach; pancreatic and lung models show that arrays can be optimized, but attenuation and anatomical variation remain important. | Abdominal delivery is physically plausible and can be modeled. | Gastric-wall dose-response, dynamic effects of filling or ascites, or gastric-tumor coverage. | L1 | [23, 25, 32] |
| Combination rationale | Membrane permeability and impaired DNA repair provide a mechanistic rationale for chemotherapy combinations. General comparison: electrically assisted drug-delivery approaches provide a broader physical context, not empirical evidence for gastric TTFields regimens. | Supports prospective testing with predefined timing and readouts. | Does not establish clinical efficacy or the best regimen in gastric cancer. | L1–L2 | [98, 100, 107] |

Percentages denote the remaining values relative to control, not percentage reductions. Overall effect is the source-reported composite of cell count and colony-forming ability; the reported values are retained without recomputation from rounded summary percentages. Colony formation was assessed after the 72-h TTFields exposure.

The indications are situated in different positions. Glioblastoma, malignant pleural mesothelioma, metastatic NSCLC, and locally advanced pancreatic adenocarcinoma have received regulatory approval; however, the maturity of evidence varies, with GBM having the most comprehensive data. PANOVA-3 facilitated regulatory approval in pancreatic cancer, although the improvement in OS was modest—16.2 versus 14.2 months (HR 0.82, 95% CI 0.68–0.99) [8]. Additional research is needed on guideline adoption, real-world access, and subgroup selection. NSCLC brain metastases post-SRS, gynecological tumors, and gastric cancer remain in exploratory or translational phases; METIS met its primary endpoint of time to intracranial progression [118]. Interpretation should account for competing non-neurologic mortality, systemic disease and its treatment, and device usage; intracranial control should not be equated with an overall-survival benefit. No peer-reviewed outcome paper exists for gastric cancer. The NCT04281576 registry and the Annals of Oncology LBA3 abstract describe the same single-arm phase II EF-31 study. As of 24 July 2026, the registry lacked a structured results module, and the abstract only presented an exploratory patient signal [10, 11]. These findings support further exploration but do not establish gastric cancer as a mature clinical application.

Glioblastoma currently has the most comprehensive evidence for TTFields. The EF-14 dosimetry analysis provides a retrospective quantitative association between modeled delivery, device usage, and survival [30], and greater monthly device use is also associated with longer survival [119]. Because adherence is embedded in LMiDD, the adjusted association remains susceptible to residual confounding and is not independent confirmation of a biophysical causal chain; validation beyond the original analysis population is required. Separately, the randomized EF-14 trial reported median OS of 20.9 versus 16.0 months [5]. The randomized treatment comparison should not be conflated with the nonrandomized dosimetry and adherence analyses. Box 2 summarizes the exposure characterization, thermal controls, orthogonal validation, and adherence-related checks used to assess the credibility of these links. Negative or limited results also reflect on the stage of research; EF-11 found no survival benefit over chemotherapy in recurrent GBM [3], and early pancreatic studies highlighted practical challenges in delivery and efficacy [40].

The upcoming research tasks include developing improved biological readouts, implementing causal screening, and conducting extracranial dosimetry. Single-cell SERS platforms enable monitoring responses over time rather than just at a single endpoint [65, 67]. Genome-wide functional screens can distinguish between purely descriptive transcriptional changes and actual causal targets. The detection of a miRNA sensitivity signal in primary GBM cultures indicates that biomarker studies should also assess susceptibility prior to field exposure [120]. Multiphysics models incorporating anatomical

heterogeneity, fluid dynamics, and anisotropy could enhance dose calibration between the brain and torso, with automated personalized modeling as one promising approach [24]. Additionally, combination therapies should have predefined schedules and partner selection criteria, especially when involving immune therapy and DNA-damage-response strategies.

Delivery engineering tackles issues such as deep-field attenuation, skin-heating limits, anatomical changes, and long-term device load. Techniques like multidirectional excitation and pulsed protocols seek to enhance directional coverage, instantaneous intensity, and energy efficiency [38, 39]. Intracranial coupled electrodes aim to minimize attenuation through the scalp and skull while enabling directional control [121]. Ultrasound-activated piezoelectric nanofibres are being investigated for wireless local field generation [122]. These represent the next generation of delivery methods, though they currently have much lower evidence maturity compared to wearable systems tested in randomized trials. They should not be marketed as current clinical options.

The framework presents three testable predictions. First, if dielectrophoresis significantly influences the clinical effect, then orientation sequences optimized based on local spindle-axis distributions and cell-size-frequency matching should outperform those that match intensity but ignore orientation. A lack of such results would weaken the mechanical explanation as a key clinical factor. Second, if the transcriptional fingerprint is a shared causal program instead of merely a consequence of strong mitotic arrest, comparing it with unrelated antimitotic drugs should distinguish a common arrest component from a TTFields-specific component (Section 4.3). Third, if the dose-survival relationship mainly reflects the treatment mechanism rather than confounding from adherence, it should remain significant after controlling for time-varying performance status or in a credible sham-controlled study (Section 8). None of these predictions have been directly tested yet, and doing so will require planned, measured field doses, *in vivo* mediating biomarkers, and site-specific extracranial calibration.

## 8. Limitations

Two types of limitations need to be considered separately. Section 8.1 addresses the evidence, including model fidelity, generalizability, clinical design, and source independence. Section 8.2 focuses on the methods employed in this narrative review.

### 8.1 Constraints of the evidence base

**Computational assumptions often rely on population-average dielectric values and tend to simplify tissue anisotropy.** While phantom experiments offer validation, there are no available spatial field measurements in actual patients [27]. The dose-survival thresholds referenced here were established in the brain [30] and have not been tailored for extracranial regions. Additionally, studies on the pancreas demonstrate that achieving an appropriate computed field does not necessarily ensure a biological response [40].

**The generalizability of nanomechanical and single-cell data remains limited.** The most direct nanomechanical measurement of a TTFields effect has been demonstrated in only one tumor type [51]. Wide replication of real-time single-cell platforms has not yet occurred [65]. Additionally, the proposed direct dielectrophoretic action on microtubules has been challenged at clinical field strengths [46]. Current data do not clarify whether the cross-cancer transcriptional fingerprint indicates a shared causal mechanism or a response converging to mitotic stress [75].

**Clinical credibility depends on evaluating evidence based on study design, approval status, and risk of bias.** Study designs vary from randomized phase 3 trials like EF-14, LUNAR, and PANOVA-3 [5, 8], to the single-arm STELLAR study [6], and include real-world cohorts and preclinical research [9, 109]. Approved uses encompass glioblastoma, mesothelioma, metastatic NSCLC, and locally advanced pancreatic cancer. Ongoing evidence generation is needed for brain metastases, gynecological tumors, and gastric cancer. Three main challenges influence interpretation: first, the wearable field-generating array is hard to mask with a convincing sham, risking open-label bias; second, outcome assessment is linked to roughly 18 hours of daily device use, complicating adherence and dosage analysis; third, clinical benefit is more established than demonstrating a direct causal pathway from mechanism to outcome.

**Confounding from adherence.** Device use correlated with improved EF-14 outcomes [119], and dosimetric analysis linked simulated dose to survival [30]. While these support a treatment effect, healthy-adherer bias suggests the same association might result from other factors. Patients able to wear a cranial array for about 18 hours daily likely differ in performance status, caregiver support, and disease progression compared to those with less use. An open-label, sham-less study cannot definitively distinguish these factors from a true dose effect. Current data do not specify how much of the survival difference is due to this bias. Without quantitative bias analysis, time-varying adjustments, or a credible sham control, the relation between usage and outcome should not be

viewed as evidence of causality. Additionally, the dosimetric threshold, derived from a single retrospective simulation cohort, needs prospective validation.

**Access, device burden, and abdominal use must be considered.** Non-invasive treatments are not always low burden. Factors like frequent daily use, regular array replacements, power management, skin reactions, and contact with support services influence access and adherence. Abdominal use adds complexity with variables such as body shape, posture, gastrointestinal filling, ascites, incisions or stomas, skin folds, sweating, and mobility. Patients with advanced gastric cancer may also face malnutrition, cachexia, pain, ascites, or gastrointestinal symptoms. Therefore, acceptability cannot be assumed based solely on GBM or thoracic indications. Future gastric-cancer studies should also evaluate cost, reimbursement, caregiver support, maintenance, travel, and work as part of feasibility outcomes.

**Transfer of field computation across different anatomical sites is theoretically feasible, but brain-specific dose thresholds are not transferable.** Effects like antimitotic activity and membrane permeability may be more universal, whereas blood-brain barrier modulation remains regionally specific. The extensive evidence for GBM has no equivalent outside the brain.

In gastric cancer, AGS and KATO III experiments support *in vitro* responses to 150 kHz TTFields and their combination with FOLFOX [9]. Clinical evidence is limited to the single-arm phase II EF-31 study, represented by its registry record and conference abstract rather than two independent studies [10, 11]. These sources do not establish gastric-tumor dose–response calibration or controlled patient benefit. Whether clinically usable surface arrays can maintain target coverage across changing gastric contents and geometry remains unresolved (Section 2.3). Brain-derived thresholds and barrier mechanisms should therefore remain site-specific until validated elsewhere.

The independence of the evidence base warrants consideration, because some mechanistic and clinical TTFields studies were conducted or funded by Novocure and its partners. While this does not discredit individual studies, it could affect the framing of research questions, the reporting of negative results, and publication chances. Independent replication becomes especially crucial for significant nanomechanical and multi-omic discoveries that rely on a single source.

**Scope.** This review focuses solely on TTFields-type intermediate-frequency alternating electric fields. It does not draw conclusions from nanosecond pulsed fields, irreversible electroporation, static fields, or low-frequency magnetic fields. Research with poorly defined exposure parameters, lacking thermal controls, or unverified field delivery was considered less reliable. The strongest evidence is found where physical dose and clinical outcomes are directly measured, while the weakest is where causality across different scales is only inferred.

### 8.2 Limitations of this review

**This is a narrative rather than a systematic review.** It aimed to synthesize mechanisms and evidence across different scales. However, it did not follow a registered protocol or a formal, fully reproducible process for inclusion and exclusion. As a result, study selection relied on the authors' judgment, and the review's coverage cannot be considered comprehensive.

**Selection and language bias may influence the findings.** Without a predefined protocol, it's impossible to rule out selection and publication bias. Positive or unusual results are often more likely to be found and published than negative ones. The search primarily targeted English-language sources, potentially missing evidence in other languages. These biases were not measured.

**Author-proposed maturity grading.** The two-track framework—combining L0–L3 mechanistic and cross-scale maturity grading with a separate clinical evidence record—is an author-proposed heuristic for this review, not a validated clinical scoring tool or established guideline.

## 9. Conclusion

The effects of TTFields have been observed in aspects such as field distribution, cellular mechanics, molecular responses, and patient outcomes. However, these findings do not yet establish a complete causal sequence. The main quantitative clinical dose–outcome signal remains the retrospective association between simulated tumor-bed dose and survival in the EF-14 glioblastoma cohort [30], which should be interpreted as a post hoc, adherence-incorporating correlation rather than an independently validated causal dose threshold. Connections from field exposure to changes in the cytoskeleton, from cytoskeletal alterations to the molecular state of individual cells, and from molecular state to survival are supported by separate studies at each scale, but lack *in vivo* mediating measurements. Therefore, this framework is a testable organizational hypothesis rather than an established mechanistic pathway. It highlights missing measurements and suggests a simpler explanation involving both direct antimitotic effects and confounding factors related to adherence

contributing to clinical outcomes. Currently, TTFields are described as working through multiple mechanisms, but whether these are part of a single causal pathway remains uncertain.

Two research priorities are identified. Firstly, field dose should be viewed as a planned and verifiable treatment parameter. While the retrospective dose-survival connection in glioblastoma offers a starting point [30], there is no site-specific extracranial calibration available. *In vitro* data on gastric cancer support testing 150 kHz TTFields with FOLFOX, but measurements of gastric-wall or abdominal field distribution, along with animal dose-response studies and patient outcomes, are still needed [9]. Secondly, combination studies must specify the mechanism and timing beforehand. Reversible membrane permeabilization provides a rationale for improving chemotherapy uptake, whereas BBB modulation offers a CNS-specific drug-delivery rationale [98, 101]. Impaired DNA repair supports testing combinations with radiotherapy and DNA-repair inhibitors [94, 104]. Separately, preclinical evidence of immunogenic cell death and immune activation supports combinations with immune-checkpoint inhibitors [82, 115, 116]. These rationales require indication-specific validation. Advances in NSCLC and locally advanced pancreatic cancer regulation support ongoing development of such combinations. For gastric cancer, further translation requires abdominal dosimetry, evaluation of patient burden, animal experiments, and controlled clinical endpoints.

The Scale-Maturity Grading shown in Box 1 is a heuristic suggested by the authors, not yet validated as a formal tool. While macroscopic dosimetry and GBM clinical evidence are more developed, nanomechanical, multi-omic, and resistance research offer mainly descriptive insights with limited evidence of causal links across different scales. Future research should aim to identify consistent molecular programs across various cancers, establish dose-response relationships beyond the brain, and investigate whether immunogenic and mechanotransductive changes initiate or result from treatment responses. These findings will clarify if TTFields can evolve from a generally effective treatment to a personalized bioelectronic therapy.

**Box 1. Separating mechanistic and cross-scale evidence from clinical evidence status**

This author-proposed framework records two distinct evidence dimensions. Dimension 1 grades mechanistic and cross-scale evidence (L0–L3) for specific mechanisms or scale-to-scale links in a defined model, exposure condition, and readout. Dimension 2 records clinical study design, endpoints, and regulatory status separately; it is not a mechanistic L4 rung. A positive clinical endpoint does not establish the intervening mechanism, and no single maturity score is assigned to an entire indication.

Dimension 1 — Mechanistic and cross-scale evidence maturity (L0–L3, applied to specific mechanisms or scale-to-scale links).

**Table 6:** Framework levels

| Level | Definition | Evidence required to assign this level |
|---|---|---|
| L0, Phenomenological observation | An exposure-associated effect is observed. | At least one study reports the effect, but a quantitative parameter–response relationship and causal mechanism have not been established. |
| L1, Quantitative dose–response | A response is measured across relevant field parameters. | Characterized exposure and appropriate controls support a quantitative relation involving frequency, intensity, or orientation. Frequency-dependent responses need not be monotonic; this level alone does not establish a molecular mechanism. |
| L2, Mechanistic anchoring | A specified mechanism has functional support in the tested model. | Loss- or gain-of-function, inhibition, or another functional perturbation changes the effect, with controls addressing alternative explanations. Support is restricted to the tested model and exposure conditions. |
| L3, Cross-scale predictive bridge | An explicit quantitative mapping predicts an outcome at another scale. | Predictive performance is evaluated in at least one independent dataset and major confounders, including adherence where relevant, are addressed. Predictive association alone is not proof of an independent causal mechanism without L2 functional-perturbation support and adequate control of confounding. |

Dimension 2 — Clinical evidence status (recorded separately; not a mechanistic L4 rung).

For the clinical track, report study design, population, regimen, endpoint findings, reporting status, and regulatory authorization. A randomized clinical benefit may coexist with unresolved mechanisms. Multiple records of the same trial, including the EF-31 registry and conference abstract, are not independent replications.

For mechanistic assignments, record the supporting source, model, exposure, readout, and criterion met. Use the highest level whose full criteria are supported; use not assessable when the criteria cannot be evaluated. Field-delivery feasibility alone is engineering evidence, not proof of a biological mechanism. An independently validated prediction without L2 functional perturbation and adequate confounder control remains predictive rather than independent causal proof.

Within the evidence included in this review, no TTFields cross-scale link meets the L3 criteria. Macroscopic modeling and dose–outcome evidence are summarized within an L1–L2 range, but the EF-14 LMiDD–survival association is a post hoc modeled correlation from a single cohort, incorporates device-

use adherence, and lacks independent multi-cohort validation; it is not an L3 bridge or independent L2 causal proof. Nanomechanical and multi-omic findings remain predominantly descriptive or parameter–response evidence; specific resistance and sensitization mechanisms can receive L2 only where functional perturbation supports the stated mechanism. Gastric-cancer mechanistic evidence remains preclinical L1. The EF-31 exploratory single-arm phase II signal is recorded only on the clinical track, not assigned a mechanistic grade.

**Box 2. Validation and credibility toolkit.**

A checklist for identifying true field effects versus artifacts and confounds:

- Use orthogonal controls for any "direct" mechanism claims, as indirect or thermal pathways may mimic non-thermal effects.
- Report temperature and dose measurements alongside biological results.
- Verify *in vivo* field distribution, not just phantom validation.
- Inclusion criteria should specify the frequency, intensity, iso-thermal conditions, and confirmed field delivery; studies with weak parameters should be deprioritized.
- Separate device-use adherence (hours per day) from modeled field intensity ($|E|$) and power loss density (LMiPD), rather than relying solely on composite metrics such as LMiDD that multiply simulated physical dose by compliance.

**Box 3. An estimate of the force on the spindle based on scaling principles (mechanics of the mechanical rung).**

The framework's title mentions bioelectric–mechanical coupling, and this section outlines, in approximate terms, what the coupling must overcome:

- Single-dimer interaction energy versus thermal energy. Using the representative free-dimer value $p = 3000\ D \approx 1.00 \times 10^{-26}\ C \cdot m$ [44], a reference field magnitude $E = 200\ V/m$ gives $pE \approx 2.00 \times 10^{-24}\ J$. With $k_B = 1.380649 \times 10^{-23}\ J/K$ and $T = 310\ K$, $k_BT \approx 4.28 \times 10^{-21}\ J$ and $pE/k_BT \approx 4.7 \times 10^{-4}$. This is an illustrative energy-scale comparison, not a direct measurement of force or a calculation of the cycle-averaged response to TTFields.
- Two amplifiers are necessary for the mechanism: (i) cooperativity—an assembling microtubule exposes $10^2$–$10^3$ partially co-oriented dimers; (ii) field intensification at the cleavage furrow—the narrowing conductive cross-section during cytokinesis concentrates the current density, and dielectrophoretic force, which $\propto \nabla|E|^2$, increases steeply with this concentration [2, 44].
- Current status. Both amplifiers are physically plausible, but neither has been directly measured in a dividing cell. Therefore, the link between the field and spindle disruption is theoretical rather than demonstrated, which is why the nanomechanical scale is graded L1 (Box 1), and why the dissenting electrodynamic perspective [46] remains a relevant alternative rather than a footnote.

This section directly addresses the question posed in the Introduction: how a force at the single-cell level could be amplified, and its honest conclusion is that such amplification is plausible but not yet proven.

## Abbreviations

TTFields: Tumor Treating Fields
GBM: glioblastoma
OS: overall survival
GEJ: gastroesophageal-junction
UPR: unfolded-protein response
AP: anterior-posterior
LR: left-right
PFS: progression-free survival
HR: hazard ratio
SRS: stereotactic radiosurgery
HDE: Humanitarian Device Exemption
PMA: premarket approval
LMiDD: local minimum dose density
LMiPD: local minimum power density
AFM: atomic force microscopy
BBB: blood–brain barrier
CNS: central nervous system
NSCLC: non-small-cell lung cancer
FDA: U.S. Food and Drug Administration
4D-CT: four-dimensional computed tomography
MRI: magnetic resonance imaging
SERS: Surface-enhanced Raman spectroscopy

## Acknowledgements

We thank BioRender. The figures were created using BioRender (https://biorender.com).

### Funding statement

This research was funded by the Shaanxi Province Postdoctoral Fund (No. 2023BSHYDZZ140), the Shaanxi Polytechnic University Doctoral Startup Funding (No. BSJ-2023-05).

### Author contributions

YWY contributed to writing—original draft. HHZ and YPZ — formal analysis. YLS— data curation. JFZ and HJL—review and editing, writing—

original draft, validation, supervision. All authors reviewed the results and approved the final version of the manuscript.

### Use of large language models, AI and machine learning tools

During the preparation of this manuscript, the authors used large language model tools solely for language polishing and readability improvement. No purely AI-generated content is included. The authors reviewed and edited all text and take full responsibility for the content of the publication.

## Competing Interests

The authors have declared that no competing interest exists.

## References


1. Kirson ED, Gurvich Z, Schneiderman R, Dekel E, Itzhaki A, Wasserman Y, et al. Disruption of Cancer Cell Replication by Alternating Electric Fields. Cancer research. 2004; 64: 3288-95.
2. Kirson ED, Dbalý V, Tovaryš F, Vymazal J, Soustiel JF, Itzhaki A, et al. Alternating electric fields arrest cell proliferation in animal tumor models and human brain tumors. Proceedings of the National Academy of Sciences. 2007; 104: 10152-7.
3. Stupp R, Wong ET, Kanner AA, Steinberg D, Engelhard H, Heidecke V, et al. NovoTTF-100A versus physician's choice chemotherapy in recurrent glioblastoma: A randomised phase III trial of a novel treatment modality. European Journal of Cancer. 2012; 48: 2192-202.
4. Stupp R, Taillibert S, Kanner AA, Kesari S, Steinberg DM, Toms SA, et al. Maintenance Therapy With Tumor-Treating Fields Plus Temozolomide vs Temozolomide Alone for Glioblastoma. JAMA. 2015; 314: 2535.
5. Stupp R, Taillibert S, Kanner A, Read W, Steinberg DM, Lhermitte B, et al. Effect of Tumor-Treating Fields Plus Maintenance Temozolomide vs Maintenance Temozolomide Alone on Survival in Patients With Glioblastoma. JAMA. 2017; 318: 2306.
6. Ceresoli GL, Aerts JG, Dziadziuszko R, Ramlau R, Cedres S, van Meerbeeck JP, et al. Tumour Treating Fields in combination with pemetrexed and cisplatin or carboplatin as first-line treatment for unresectable malignant pleural mesothelioma (STELLAR): a multicentre, single-arm phase 2 trial. The Lancet Oncology. 2019; 20: 1702-9.
7. Leal T, Kotecha R, Ramlau R, Zhang L, Milanowski J, Cobo M, et al. Tumor Treating Fields therapy with standard systemic therapy versus standard systemic therapy alone in metastatic non-small-cell lung cancer following progression on or after platinum-based therapy (LUNAR): a randomised, open-label, pivotal phase 3 study. The Lancet Oncology. 2023; 24: 1002-17.
8. Babiker HM, Picozzi V, Chandana SR, Melichar B, Kasi A, Gang J, et al. Tumor Treating Fields With Gemcitabine and Nab-Paclitaxel for Locally Advanced Pancreatic Adenocarcinoma: Randomized, Open-Label, Pivotal Phase III PANOVA-3 Study. Journal of Clinical Oncology. 2025; 43: 2350-60.
9. Fishman H, Ene HM, Zeevi E, Flint-Brodsly N, Wainer-Katsir K, Frechtel-Gerzi R, et al. Tumor Treating Fields (TTFields), and their concomitant application with FOLFOX, are effective for the treatment of gastric cancer cells. Front Oncol. 2026; 16: 1575083.
10. National Library of Medicine (US). Effect of Tumor Treating Fields (TTFields, 150 kHz) Concomitant with Chemotherapy as First Line Treatment of Unresectable Gastroesophageal Junction or Gastric Adenocarcinoma. ClinicalTrials.gov **2024**. NCT04281576; first posted February 24, 2020; last update posted November 14, 2024. Available at: https://clinicaltrials.gov/study/NCT04281576. Accessed October 15, 2026.
11. Li J, Cang S, Ling Y, Lam KO, Chen Y, Xu Y, et al. Tumor Treating Fields (TTFields) therapy plus XELOX chemotherapy for front line treatment of advanced unresectable gastroesophageal junction adenocarcinoma (GEJC) or gastric adenocarcinoma (GC): A multicenter phase II trial. Annals of Oncology. 2022; 33: S1455-S.
12. Aguilar AA, Ho MC, Chang E, Carlson KW, Natarajan A, Marciano T, et al. Permeabilizing Cell Membranes with Electric Fields. Cancers. 2021; 13: 2283.
13. Moser JC, Salvador E, Deniz K, Swanson K, Tuszynski J, Carlson KW, et al. The Mechanisms of Action of Tumor Treating Fields. Cancer research. 2022; 82: 3650-8.
14. Rominiyi O, Vanderlinden A, Clenton SJ, Bridgewater C, Al-Tamimi Y, Collis SJ. Tumour treating fields therapy for glioblastoma: current advances and future directions. British journal of cancer. 2020; 124: 697-709.
15. Hong P, Kudulaiti N, Wu S, Nie J, Zhuang D. Tumor treating fields: a comprehensive overview of the underlying molecular mechanism. Expert Review of Molecular Diagnostics. 2021; 22: 19-28.
16. Shams S, Patel CB. Anti-cancer mechanisms of action of therapeutic alternating electric fields (tumor treating fields [TTFields]). Journal of Molecular Cell Biology. 2022; 14.
17. Gabriel S, Lau RW, Gabriel C. The dielectric properties of biological tissues: III. Parametric models for the dielectric spectrum of tissues. Physics in Medicine and Biology. 1996; 41: 2271-93.
18. Gabriel S, Lau RW, Gabriel C. The dielectric properties of biological tissues: II. Measurements in the frequency range 10 Hz to 20 GHz. Physics in Medicine and Biology. 1996; 41: 2251-69.
19. Gabriel C, Gabriel S, Corthout E. The dielectric properties of biological tissues: I. Literature survey. Physics in Medicine and Biology. 1996; 41: 2231-49.
20. Wenger C, Salvador R, Basser PJ, Miranda PC. The electric field distribution in the brain during TTFields therapy and its dependence on tissue dielectric properties and anatomy: a computational study. Physics in Medicine and Biology. 2015; 60: 7339-57.
21. Miranda PC, Mekonnen A, Salvador R, Basser PJ. Predicting the electric field distribution in the brain for the treatment of glioblastoma. Physics in Medicine and Biology. 2014; 59: 4137-47.
22. Wenger C, Miranda PC, Salvador R, Thielscher A, Bomzon Z, Giladi M, et al. A Review on Tumor-Treating Fields (TTFields): Clinical Implications Inferred From Computational Modeling. IEEE Reviews in Biomedical Engineering. 2018; 11: 195-207.
23. Zheng M, Wang Y, Chen S, Suo Y, Yu J, Zhang X. Enhancing Electric Field Distribution in the Pancreas for Improved TTFields Therapy: A Computational Modeling Investigation. IEEE Trans Biomed Eng. 2024; 71: 2612-9.
24. Xie X, Fan Z, Mou H, Lan Y, Wang Y, Wang M, et al. AutoSimTTF: a fully automatic pipeline for personalized electric field simulation and treatment planning of tumor treating fields. Physics in Medicine & Biology. 2026; 71: 045004.
25. Zhang K, Chen S, Zheng M, Suo Y, Yu J, Zhang X. Computational Simulation and Experimental Validation of Electric Field Distribution Patterns in TTFields Therapy for Lung Cancer. Bioelectromagnetics. 2026; 47: e70064.
26. Xiao Y, Chen C, Xia J, Zheng Y, Wang L, Lu M, et al. Tumor Treating Fields: A Review of Computational Strategies for Thermal Safety and Personalization Treatment. IEEE Trans Biomed Eng. 2026; 73: 2199-213.
27. Ma M, Fu G, Wang M, Liu H, Zheng D, Pan Y, et al. Validation of Computational Simulation for Tumor-treating Fields with Homogeneous Phantom. 2022 44th Annual International Conference of the IEEE Engineering in Medicine & Biology Society (EMBC). 2022: 975-8.
28. Wong ET, Lok E. Body Fluids Modulate Propagation of Tumor Treating Fields. Advances in Radiation Oncology. 2024; 9: 101316.
29. Nguyen H, Schubert KE, Pohling C, Chang E, Yamamoto V, Zeng Y, et al. Impact of glioma peritumoral edema, tumor size, and tumor location on alternating electric fields (AEF) therapy in realistic 3D rat glioma models: a computational study. Physics in Medicine & Biology. 2024; 69: 085015.
30. Ballo MT, Urman N, Lavy-Shahaf G, Grewal J, Bomzon Ze, Toms S. Correlation of Tumor Treating Fields Dosimetry to Survival Outcomes in Newly Diagnosed Glioblastoma: A Large-Scale Numerical Simulation-Based Analysis of Data from the Phase 3 EF-14 Randomized Trial. International Journal of Radiation Oncology*Biology*Physics. 2019; 104: 1106-13.
31. Mikic N, Gentilal N, Cao F, Lok E, Wong ET, Ballo M, et al. Tumor-treating fields dosimetry in glioblastoma: Insights into treatment planning, optimization, and dose–response relationships. Neuro-Oncology Advances. 2024; 6.
32. Blatt R, Davidi S, Munster M, Shteingauz A, Cahal S, Zeidan A, et al. In Vivo Safety of Tumor Treating Fields (TTFields) Applied to the Torso. Frontiers in Oncology. 2021; 11.
33. Korshoej AR, Hansen FL, Mikic N, von Oettingen G, Sørensen JCH, Thielscher A. Importance of electrode position for the distribution of tumor treating fields (TTFields) in a human brain. Identification of effective layouts through systematic analysis of array positions for multiple tumor locations. PloS one. 2018; 13: e0201957.
34. Wenger C, Salvador R, Basser PJ, Miranda PC. Improving Tumor Treating Fields Treatment Efficacy in Patients With Glioblastoma Using Personalized Array Layouts. International Journal of Radiation Oncology*Biology*Physics. 2016; 94: 1137-43.
35. Chaudhry A, Benson L, Varshaver M, Farber O, Weinberg U, Kirson E, et al. NovoTTF™-100A System (Tumor Treating Fields) transducer array layout planning for glioblastoma: a NovoTAL™ system user study. World Journal of Surgical Oncology. 2015; 13.
36. Cao F, Mikic N, Wong ET, Thielscher A, Korshoej AR. Guidelines for Burr Hole Surgery in Combination With Tumor Treating Fields for Glioblastoma: A Computational Study on Dose Optimization and Array Layout Planning. Frontiers in Human Neuroscience. 2022; 16.
37. Lok E, Liang O, Haack M, Wong ET. Hydrogel and scalp/skin conductivities impact dose from tumor treating fields. Frontiers in Bioengineering and Biotechnology. 2025; 13.
38. Zhao Y, Yue S, Fu K. A parameter computation and optimization method in multi-directional exciting tumor treating fields. Comput Methods Programs Biomed. 2026; 285: 109545.
39. Lv Y, Lu S, Wang H, Zhang J, Chen C. A Pulsed Tumor Treating Fields Protocol to Improve Glioblastoma Therapy. IEEE Trans Biomed Eng. 2026; 73: 2474-83.

40. Pfeifer T, Bai L, Gladkich J, Gross W, Liu L, Herr I, et al. Therapy of pancreatic cancer with alternating electric fields: Limitations of the method. Bioelectrochemistry (Amsterdam, Netherlands). 2021; 141: 107881.
41. Hershkovich HS, Urman N, Yesharim O, Naveh A, Bomzon Ze. The dielectric properties of skin and their influence on the delivery of tumor treating fields to the torso: a study combining in vivo measurements with numerical simulations. Physics in Medicine & Biology. 2019; 64: 185014.
42. Giladi M, Schneiderman RS, Voloshin T, Porat Y, Munster M, Blat R, et al. Mitotic Spindle Disruption by Alternating Electric Fields Leads to Improper Chromosome Segregation and Mitotic Catastrophe in Cancer Cells. Scientific reports. 2015; 5.
43. Gera N, Yang A, Holtzman TS, Lee SX, Wong ET, Swanson KD. Tumor Treating Fields Perturb the Localization of Septins and Cause Aberrant Mitotic Exit. PloS one. 2015; 10: e0125269.
44. Tuszynski J, Wenger C, Friesen D, Preto J. An Overview of Sub-Cellular Mechanisms Involved in the Action of TTFields. International Journal of Environmental Research and Public Health. 2016; 13: 1128.
45. Timmons JJ, Preto J, Tuszynski JA, Wong ET. Tubulin's response to external electric fields by molecular dynamics simulations. PloS one. 2018; 13: e0202141.
46. Li X, Liu K, Fang H, Liu Z, Tang Y, Dai P. Electrodynamic interaction between tumor treating fields and microtubule electrophysiological activities. APL Bioengineering. 2024; 8.
47. Cross SE, Jin Y-S, Rao J, Gimzewski JK. Nanomechanical analysis of cells from cancer patients. Nature Nanotechnology. 2007; 2: 780-3.
48. Plodinec M, Loparic M, Monnier CA, Obermann EC, Zanetti-Dallenbach R, Oertle P, et al. The nanomechanical signature of breast cancer. Nature Nanotechnology. 2012; 7: 757-65.
49. Otto O, Rosendahl P, Mietke A, Golfier S, Herold C, Klaue D, et al. Real-time deformability cytometry: on-the-fly cell mechanical phenotyping. Nature methods. 2015; 12: 199-202.
50. Persano F, Parodi A, Pallaeva T, Kolesova E, Zamyatnin AA, Pokrovsky VS, et al. Atomic Force Microscopy: A Versatile Tool in Cancer Research. Cancers. 2025; 17: 858.
51. Kulkarni T, Banik S, Mukhopadhyay D, Babiker H, Bhattacharya S. Tumor-Treating Fields Alter Nanomechanical Properties of Pancreatic Ductal Adenocarcinoma Cells Co-Cultured with Extracellular Matrix. Journal of Functional Biomaterials. 2025; 16: 160.
52. Dupont S, Morsut L, Aragona M, Enzo E, Giulitti S, Cordenonsi M, et al. Role of YAP/TAZ in mechanotransduction. Nature. 2011; 474: 179-83.
53. Piccolo S, Dupont S, Cordenonsi M. The Biology of YAP/TAZ: Hippo Signaling and Beyond. Physiological Reviews. 2014; 94: 1287-312.
54. Zanconato F, Cordenonsi M, Piccolo S. YAP/TAZ at the Roots of Cancer. Cancer Cell. 2016; 29: 783-803.
55. Levental KR, Yu H, Kass L, Lakins JN, Egeblad M, Erler JT, et al. Matrix Crosslinking Forces Tumor Progression by Enhancing Integrin Signaling. Cell. 2009; 139: 891-906.
56. Kechagia JZ, Ivaska J, Roca-Cusachs P. Integrins as biomechanical sensors of the microenvironment. Nature Reviews Molecular Cell Biology. 2019; 20: 457-73.
57. Zhu B, Li F, Yu J, Liang Z, Ke X, Wang Y, et al. PIEZO1 mediates matrix stiffness-induced tumor progression in kidney renal clear cell carcinoma by activating the Ca2+/Calpain/YAP pathway. Biochimica et Biophysica Acta (BBA) - Molecular Cell Research. 2025; 1872: 119871.
58. Chen X, Xu Z, Tang K, Hu G, Du P, Wang J, et al. The Mechanics of Tumor Cells Dictate Malignancy via Cytoskeleton-Mediated APC/Wnt/β-Catenin Signaling. Research. 2023; 6.
59. Voloshin T, Schneiderman RS, Volodin A, Shamir RR, Kaynan N, Zeevi E, et al. Tumor Treating Fields (TTFields) Hinder Cancer Cell Motility through Regulation of Microtubule and Actin Dynamics. Cancers. 2020; 12: 3016.
60. Kim EH, Song HS, Yoo SH, Yoon M. Tumor treating fields inhibit glioblastoma cell migration, invasion and angiogenesis. Oncotarget. 2016; 7: 65125-36.
61. Silginer M, Weller M, Stupp R, Roth P. Biological activity of tumor-treating fields in preclinical glioma models. Cell Death & Disease. 2017; 8: e2753-e.
62. Naggay BK, Farahani SK, Gao X, Holle A, Kemkemer R. Direct current electrical fields inhibit cancer cell motility in microchannel confinements. Scientific reports. 2025; 15.
63. Li X, Wang J. Mechanical tumor microenvironment and transduction: cytoskeleton mediates cancer cell invasion and metastasis. International Journal of Biological Sciences. 2020; 16: 2014-28.
64. Kirson ED, Giladi M, Gurvich Z, Itzhaki A, Mordechovich D, Schneiderman RS, et al. Alternating electric fields (TTFields) inhibit metastatic spread of solid tumors to the lungs. Clinical & Experimental Metastasis. 2009; 26: 633-40.
65. Yu K, Chen S, Zhu R. Spatial-Temporal Multiomics Profiling of Living Single Cells on Chip for Cancer Therapy. ACS sensors. 2025; 10: 7497-507.
66. Sun D, Cao F, Tian Y, Li A, Xu W, Chen Q, et al. Label-Free Detection of Multiplexed Metabolites at Single-Cell Level via a SERS-Microfluidic Droplet Platform. Anal Chem. 2019; 91: 15484-90.
67. Liu F, Liu J, Luo Y, Wu S, Liu X, Chen H, et al. A Single-Cell Metabolic Profiling Characterizes Human Aging via SlipChip-SERS. Advanced Science. 2024; 11.
68. Chen K, Wang Z. A Micropillar Array Based Microfluidic Device for Rare Cell Detection and Single-Cell Proteomics. Methods and Protocols. 2023; 6: 80.
69. Szymborski TR, Czaplicka M, Nowicka AB, Trzcińska-Danielewicz J, Girstun A, Kamińska A. Dielectrophoresis-Based SERS Sensors for the Detection of Cancer Cells in Microfluidic Chips. Biosensors. 2022; 12: 681.
70. Chen B, Gao J, Sun H, Liu Y, Zhao Y, Qiu X. Deciphering cellular heterogeneity: Breakthroughs and prospects of single-cell-level SERS analysis in precision medicine. Methods. 2025; 244: 7-29.
71. Vander Heiden MG, Cantley LC, Thompson CB. Understanding the Warburg Effect: The Metabolic Requirements of Cell Proliferation. Science. 2009; 324: 1029-33.
72. Walsh AJ, Cook RS, Manning HC, Hicks DJ, Lafontant A, Arteaga CL, et al. Optical Metabolic Imaging Identifies Glycolytic Levels, Subtypes, and Early-Treatment Response in Breast Cancer. Cancer research. 2013; 73: 6164-74.
73. Zhang C, Li J, Lan L, Cheng J-X. Quantification of Lipid Metabolism in Living Cells through the Dynamics of Lipid Droplets Measured by Stimulated Raman Scattering Imaging. Anal Chem. 2017; 89: 4502-7.
74. Feng D, Li H, Xu T, Zheng F, Hu C, Shi X, et al. High-throughput single cell metabolomics and cellular heterogeneity exploration by inertial microfluidics coupled with pulsed electric field-induced electrospray ionization-high resolution mass spectrometry. Anal Chim Acta. 2022; 1221: 340116.
75. Wainer-Katsir K, Haber A, Fishman H, Ding L, Story MD, Du R, et al. The transcriptomic fingerprint of cancer response to Tumor Treating Fields (TTFields). Cell Death Discovery. 2025; 11.
76. Chang E, Patel CB, Pohling C, Young C, Song J, Flores TA, et al. Tumor treating fields increases membrane permeability in glioblastoma cells. Cell Death Discovery. 2018; 4.
77. Canaparo R, Foglietta F, Pepa CD, Serpe L. Spotlight on membrane fluidity of normal and cancer cells: Implications for cancer diagnosis and treatment. European journal of pharmacology. 2025; 1006: 178152.
78. Xu M, Ma X, Wei T, Lu Z-X, Ren B. In Situ Imaging of Live-Cell Extracellular pH during Cell Apoptosis with Surface-Enhanced Raman Spectroscopy. Anal Chem. 2018; 90: 13922-8.
79. Obeid M, Tesniere A, Ghiringhelli F, Fimia GM, Apetoh L, Perfettini J-L, et al. Calreticulin exposure dictates the immunogenicity of cancer cell death. Nature medicine. 2006; 13: 54-61.
80. Kepp O, Senovilla L, Vitale I, Vacchelli E, Adjemian S, Agostinis P, et al. Consensus guidelines for the detection of immunogenic cell death. OncoImmunology. 2014; 3: e955691.
81. Galluzzi L, Vitale I, Warren S, Adjemian S, Agostinis P, Martinez AB, et al. Consensus guidelines for the definition, detection and interpretation of immunogenic cell death. Journal for ImmunoTherapy of Cancer. 2020; 8: e000337.
82. Voloshin T, Kaynan N, Davidi S, Porat Y, Shteingauz A, Schneiderman RS, et al. Tumor-treating fields (TTFields) induce immunogenic cell death resulting in enhanced antitumor efficacy when combined with anti-PD-1 therapy. Cancer Immunology, Immunotherapy. 2020; 69: 1191-204.
83. Chen D, Le SB, Hutchinson TE, Calinescu A-A, Sebastian M, Jin D, et al. Tumor Treating Fields dually activate STING and AIM2 inflammasomes to induce adjuvant immunity in glioblastoma. Journal of Clinical Investigation. 2022; 132.
84. Yue Y, Wang Y, Feng J, Yao M, Suo Y. Tumor treating fields suppress tumor cell growth and induce immunogenic cell death biomarkers in biliary tract cancer cell lines. Scientific reports. 2025; 15.
85. Gray GK, McFarland BC, Nozell SE, Benveniste EN. NF-κB and STAT3 in glioblastoma: therapeutic targets coming of age. Expert Review of Neurotherapeutics. 2014; 14: 1293-306.
86. Klein-Goldberg A, Voloshin T, Zemer Tov E, Paz R, Somri-Gannam L, Volodin A, et al. Role of the PI3K/AKT signaling pathway in the cellular response to Tumor Treating Fields (TTFields). Cell Death & Disease. 2025; 16.
87. Glaviano A, Foo ASC, Lam HY, Yap KCH, Jacot W, Jones RH, et al. PI3K/AKT/mTOR signaling transduction pathway and targeted therapies in cancer. Molecular cancer. 2023; 22.
88. Shteingauz A, Porat Y, Voloshin T, Schneiderman RS, Munster M, Zeevi E, et al. AMPK-dependent autophagy upregulation serves as a survival mechanism in response to Tumor Treating Fields (TTFields). Cell Death & Disease. 2018; 9.
89. Levy JMM, Towers CG, Thorburn A. Targeting autophagy in cancer. Nature Reviews Cancer. 2017; 17: 528-42.
90. Hetz C, Zhang K, Kaufman RJ. Mechanisms, regulation and functions of the unfolded protein response. Nature Reviews Molecular Cell Biology. 2020; 21: 421-38.
91. Mohamed E, Cao Y, Rodriguez PC. Endoplasmic reticulum stress regulates tumor growth and anti-tumor immunity: a promising opportunity for cancer immunotherapy. Cancer Immunology, Immunotherapy. 2017; 66: 1069-78.
92. Kessler AF, Frömbling GE, Gross F, Hahn M, Dzokou W, Ernestus R-I, et al. Effects of tumor treating fields (TTFields) on glioblastoma cells are augmented by mitotic checkpoint inhibition. Cell Death Discovery. 2018; 4.
93. Jo Y, Kim EH, Sai S, Kim JS, Cho J-M, Kim H, et al. Functional Biological Activity of Sorafenib as a Tumor-Treating Field Sensitizer for Glioblastoma Therapy. Int J Mol Sci. 2018; 19: 3684.
94. Berckmans Y, Ene HM, Ben-Meir K, Martinez-Conde A, Wouters R, Van den Ende B, et al. Tumor Treating Fields (TTFields) induce homologous recombination deficiency in ovarian cancer cells, thus mitigating drug resistance. Frontiers in Oncology. 2024; 14.
95. Davidi S, Jacobovitch S, Shteingauz A, Martinez-Conde A, Braten O, Tempel-Brami C, et al. Tumor Treating Fields (TTFields) Concomitant with Sorafenib Inhibit Hepatocellular Carcinoma In Vitro and In Vivo. Cancers. 2022; 14: 2959.
96. Kim EH, Lee WS, Oh H-K. Tumor-treating fields in combination with sorafenib curtails the growth of colorectal carcinoma by inactivating AKT/STAT3 signaling. Translational Cancer Research. 2022; 11: 2553-61.

97. Jang Y, Lee W, Sai S, Kim J, Kim J-K, Kim E. Tumor-treating fields in combination with sorafenib restrain the proliferation of liver cancer in vitro. Oncology letters. 2022; 24.
98. Koltun B, Voloshin T, David C, Kan T, Barsheshet Y, Volodin A, et al. Cancer Cell Permeability Induced by Tumor Treating Fields (TTFields) as a Physical Approach to Improve Chemotherapy Uptake and Overcome Multidrug Resistance. Molecular cancer therapeutics. 2025; 24: 1815-25.
99. Martinez-Paniagua M, Khan S, Henning NW, Konagalla SV, Patel CB. Optimized Methods to Quantify Tumor Treating Fields (TTFields)-Induced Permeabilization of Glioblastoma Cell Membranes. Methods and Protocols. 2025; 8: 10.
100. Saeed N, Coene A, Adriaens M, Ceelen W. Electric fields to enhance drug delivery to non-superficial tumors. Journal of controlled release. 2026; 395: 114931.
101. Salvador E, Kessler AF, Domröse D, Hörmann J, Schaeffer C, Giniunaite A, et al. Tumor Treating Fields (TTFields) Reversibly Permeabilize the Blood–Brain Barrier In Vitro and In Vivo. Biomolecules. 2022; 12: 1348.
102. Salvador E, Köppl T, Hörmann J, Schönhärl S, Bugaeva P, Kessler AF, et al. Tumor Treating Fields (TTFields) Induce Cell Junction Alterations in a Human 3D In Vitro Model of the Blood-Brain Barrier. Pharmaceutics. 2023; 15: 185.
103. Iv M, Naya L, Sanan S, Van Buskirk SL, Nagpal S, Thomas RP, et al. Tumor treating fields increases blood-brain barrier permeability and relative cerebral blood volume in patients with glioblastoma. The Neuroradiology Journal. 2023; 37: 107-18.
104. Giladi M, Munster M, Schneiderman RS, Voloshin T, Porat Y, Blat R, et al. Tumor treating fields (TTFields) delay DNA damage repair following radiation treatment of glioma cells. Radiation Oncology. 2017; 12.
105. Karanam NK, Srinivasan K, Ding L, Sishc B, Saha D, Story MD. Tumor-treating fields elicit a conditional vulnerability to ionizing radiation via the downregulation of BRCA1 signaling and reduced DNA double-strand break repair capacity in non-small cell lung cancer cell lines. Cell Death & Disease. 2017; 8: e2711-e.
106. Giladi M, Weinberg U, Schneiderman RS, Porat Y, Munster M, Voloshin T, et al. Alternating Electric Fields (Tumor-Treating Fields Therapy) Can Improve Chemotherapy Treatment Efficacy in Non-Small Cell Lung Cancer Both In Vitro and In Vivo. Seminars in Oncology. 2014; 41: S35-S41.
107. Fishman H, Monin R, Dor-On E, Kinzel A, Haber A, Giladi M, et al. Tumor Treating Fields (TTFields) increase the effectiveness of temozolomide and lomustine in glioblastoma cell lines. Journal of Neuro-Oncology. 2023; 163: 83-94.
108. Vanderlinden A, Jones CG, Myers KN, Rominiyi O, Collis SJ. DNA damage response inhibitors enhance tumour treating fields (TTFields) potency in glioma stem-like cells. British journal of cancer. 2023; 129: 1829-40.
109. Zhai M-l, Hu G, Shen G, Zhong Y, Huang J, Li Q, et al. Tumor treating fields combined with concurrent chemoradiotherapy for glioblastoma: A multi-institutional analysis. iScience. 2026; 29.
110. Ashmeg S, Taylor J, Lalonde R, Wadi-Ramahi S. Dosimetric impact of radiofrequency tumor treating field arrays on dose on surface and at depth. Journal of Applied Clinical Medical Physics. 2026; 27.
111. Donnini F, Battaglia G, Chibbaro S, Marampon F, Minniti G, Tini P. Tumor Treating Fields and the Glioblastoma Microenvironment: Mechanistic Convergences with Radiotherapy. Cancers. 2026; 18.
112. Vergote I, Macarulla T, Hirsch FR, Hagemann C, Miller DS. Tumor Treating Fields (TTFields) Therapy Concomitant with Taxanes for Cancer Treatment. Cancers. 2023; 15: 636.
113. Shawki MM, El Sadieque A, Elabd S, Moustafa ME. Synergetic Effect of Tumor Treating Fields and Zinc Oxide Nanoparticles on Cell Apoptosis and Genotoxicity of Three Different Human Cancer Cell Lines. Molecules. 2022; 27: 4384.
114. Bai L, Pfeifer T, Gross W, De La Torre C, Zhao S, Liu L, et al. Establishment of Tumor Treating Fields Combined With Mild Hyperthermia as Novel Supporting Therapy for Pancreatic Cancer. Frontiers in Oncology. 2021; 11.
115. Barsheshet Y, Voloshin T, Brant B, Cohen G, Koren L, Blatt R, et al. Tumor Treating Fields (TTFields) Concomitant with Immune Checkpoint Inhibitors Are Therapeutically Effective in Non-Small Cell Lung Cancer (NSCLC) In Vivo Model. Int J Mol Sci. 2022; 23: 14073.
116. Lin W, Wang Y, Li M, Feng J, Yue Y, Yu J, et al. Tumor treating fields enhance anti-PD therapy by improving CCL2/8 and CXCL9/CXCL10 expression through inducing immunogenic cell death in NSCLC models. BMC cancer. 2025; 25.
117. Wong ET, Toms SA, Ahluwalia MS. Technological Advances in the Treatment of Cancer: Combining Modalities to Optimize Outcomes. Clinical Advances in Hematology & Oncology. 2015; 13(11 Suppl 11): 3-18.
118. Mehta MP, Gondi V, Ahluwalia MS, Roberge D, Sio TTW, Trifiletti DM, et al. Tumor Treating Fields Therapy After Stereotactic Radiosurgery for Brain Metastases From Non-Small Cell Lung Cancer: Final Results of the Phase 3 METIS Study. International Journal of Radiation Oncology Biology Physics. 2026; 124: 278-93.
119. Toms SA, Kim CY, Nicholas G, Ram Z. Increased compliance with tumor treating fields therapy is prognostic for improved survival in the treatment of glioblastoma: a subgroup analysis of the EF-14 phase III trial. Journal of Neuro-Oncology. 2018; 141: 467-73.
120. Hemmer S, Henia M, Schulz-Schaeffer W, Ketter R, Landau B, Oertel J, et al. Exploratory analysis of miRNAs-21, -26a, -34a, -181c, -181d, and -485-5p as potential biomarkers for tumor treating fields sensitivity in primary glioblastoma cell cultures. Brain Tumor Pathol. 2026; 43: 85-96.
121. Yang X, Kang X, Liang T, Wu W, Xing H, Lian Y, et al. Intracranial-implanted coupled electrode tumor treating fields (ICE-TTF) enable efficient and directionally tunable electric-field delivery for glioma. Brain Stimulation. 2026; 19: 103141.
122. Dai S, Nabil A, Matsumoto Y, Abulimiti M, Sugawara Y, Ebara M. Metal-Organic Framework Composite Piezoelectric Nanofibers for Wireless Tumor Treating Fields Therapy. ACS Biomater Sci Eng. 2026; doi: 10.1021/acsbiomaterials.6c00905.